frontiers in Marine Science

ORIGINAL RESEARCH
published: 16 December 2020
doi: 10.3389/fmars.2020.576013

Stony Coral Tissue Loss Disease in Florida Is Associated With Disruption of Host–Zooxanthellae Physiology

Jan H. Landsberg[1], Yasunari Kiryu[1], Esther C. Peters[2], Patrick W. Wilson[1], Noretta Perry[1], Yvonne Waters[1], Kerry E. Maxwell[3], Lindsay K. Huebner[1] and Thierry M. Work[4]*

[1] Fish and Wildlife Research Institute, Florida Fish and Wildlife Conservation Commission, St. Petersburg, FL, United States, [2] Department of Environmental Science and Policy, George Mason University, Fairfax, VA, United States, [3] Fish and Wildlife Research Institute, Florida Fish and Wildlife Conservation Commission, Marathon, FL, United States, [4] U.S. Geological Survey, National Wildlife Health Center, Honolulu Field Station, Honolulu, HI, United States

Samples from eight species of corals (*Colpophyllia natans*, *Dendrogyra cylindrus*, *Diploria labyrinthiformis*, *Meandrina meandrites*, *Montastraea cavernosa*, *Orbicella faveolata, Pseudodiploria strigosa*, and *Siderastrea siderea*) that exhibited gross clinical signs of acute, subacute, or chronic tissue loss attributed to stony coral tissue loss disease (SCTLD) were collected from the Florida Reef Tract during 2016–2018 and examined histopathologically. The hallmark microscopic lesion seen in all eight species was focal to multifocal lytic necrosis (LN) originating in the gastrodermis of the basal body wall (BBW) and extending to the calicodermis, with more advanced lesions involving the surface body wall. This was accompanied by other degenerative changes in host cells such as mucocyte hypertrophy, degradation and fragmentation of gastrodermal architecture, and disintegration of the mesoglea. Zooxanthellae manifested various changes including necrosis (cytoplasmic hypereosinophilia, pyknosis); peripheral nuclear chromatin condensation; cytoplasmic vacuolation accompanied by deformation, swelling, or atrophy; swollen accumulation bodies; prominent pyrenoids; and degraded chloroplasts. Polyhedral intracytoplasmic eosinophilic periodic acid–Schiff-positive crystalline inclusion bodies (~1–10 μm in length) were seen only in *M. cavernosa* and *P. strigosa* BBW gastrodermis in or adjacent to active lesions and some unaffected areas (without surface lesions) of diseased colonies. Coccoidlike or coccobacilloidlike structures (Gram-neutral) reminiscent of microorganisms were occasionally associated with LN lesions or seen in apparently healthy tissue of diseased colonies along with various parasites and other bacteria all considered likely secondary colonizers. Of the 82 samples showing gross lesions of SCTLD, 71 (87%) were confirmed histologically to have LN. Collectively, pathology indicates that SCTLD is the result of a disruption of host–symbiont physiology with lesions originating in the BBW leading to detachment and sloughing of tissues from the skeleton. Future investigations could focus on identifying the cause and pathogenesis of this process.

Keywords: coral disease, histopathology, tissue loss, Florida Reef Tract, SCTLD, lytic necrosis, transmission electron microscopy

OPEN ACCESS

Edited by:
Yehuda Benayahu, Tel Aviv University, Israel

Reviewed by:
Aldo Cróquer, Simón Bolívar University, Venezuela
Michael S. Studivan, University of Miami, United States

****Correspondence:***
Jan H. Landsberg
jan.landsberg@myfwc.com

Specialty section:
This article was submitted to Coral Reef Research, a section of the journal Frontiers in Marine Science

Received: *24 June 2020*
Accepted: *19 November 2020*
Published: *16 December 2020*

Citation:
Landsberg JH, Kiryu Y, Peters EC, Wilson PW, Perry N, Waters Y, Maxwell KE, Huebner LK and Work TM (2020) Stony Coral Tissue Loss Disease in Florida Is Associated With Disruption of Host–Zooxanthellae Physiology. Front. Mar. Sci. 7:576013. doi: 10.3389/fmars.2020.576013

INTRODUCTION

The Florida Reef Tract spans some 577 km from the Dry Tortugas (the southernmost Florida Keys) to Martin County in the north. With a diverse assemblage of more than 6,000 marine species, the Florida Reef Tract attracts more than 30 million visitors annually, with fishing, diving, and boating expenditures generating more than $6.3 billion to the State.[1] This ecosystem, however, has suffered significant losses of coral and associated organisms, starting with an unexplained die-off in Panama of the dominant grazing long-spined sea urchin *Diadema antillarum* in which more than 90% of the population throughout the Caribbean was wiped out within a year (1983–1984), and populations have yet to recover (Lessios, 1988, 2016). In subsequent decades, a majority of the dominant reef coral *Acropora* (*A. palmata, A. cervicornis*) declined by about 80%, mainly due to tissue loss diseases (TLDs), leading to marked reductions in the three-dimensional complexity and biodiversity of Florida's coral reefs (Aronson and Precht, 2001). Since then, this region has experienced a plethora of coral diseases (Mueller et al., 2001; Porter et al., 2001).

Global climate change is likely to aggravate this situation. Warming temperatures induce corals to expel their dinoflagellate symbionts (zooxanthellae), a process known as bleaching (Coles and Jokiel, 1977). Since 1987, six mass coral-bleaching events have affected the entire Florida Reef Tract, with moderate intermittent incidents occurring annually since 2006 (except for 2013 when bleaching reports were low) (Manzello, 2015; Gintert et al., 2018). The Florida Reef Tract has also experienced an increasing prevalence of acute or chronic TLDs such as black-band disease, white-band disease, acroporid serratiosis, dark spot syndrome, and white plague (WP) (Kuta and Richardson, 1996; Richardson et al., 1998a,b; Patterson et al., 2002; Peters, 2015; Bruckner, 2016; Gignoux-Wolfsohn et al., 2020). The demise of acroporids, continuing intermittent chronic disease outbreaks, and coral loss due to bleaching have added to the concern over the stability and health of Florida's coral reef ecosystem (Williams and Miller, 2012) and has highlighted the previously underestimated role of disease (Miller et al., 2014).

Since 2014, an unprecedented outbreak of stony coral tissue loss disease (SCTLD), affecting more than 20 species of scleractinian corals within at least eight families, appeared to originate near Virginia Key, Miami (Precht et al., 2016). SCTLD has now spread north to Martin County and southwest to the Marquesas Keys, almost to the Dry Tortugas[2]. SCTLD has essentially encompassed most of the Florida Reef Tract with resultant sustained and widescale coral mortalities (Precht et al., 2016;[3] Walton et al., 2018; Aeby et al., 2019; Meyer et al., 2019; Rippe et al., 2019; Muller et al., 2020; Rosales et al., 2020). In 2017, SCTLD was reported in Jamaica, then in 2018 it was reported in the Mesoamerican reef system, from where it has expanded throughout the rest of the Caribbean region[4] (Alvarez-Filip et al., 2019; Weil et al., 2019[5]).

In 2014, SCTLD appeared to spread following bleaching and sedimentation events (Manzello, 2015; Miller et al., 2016), and, despite much research, the etiology of SCTLD remains unknown. Along with the diversity of species affected, SCTLD can have different rates of tissue loss, differences in lesion morphology, and differences in the distribution of lesions in a colony (Aeby et al., 2019). Subacute and chronic tissue-loss lesions can be observed with bleached borders, while acute lesions can manifest with normally pigmented tissue adjacent to denuded skeleton (Aeby et al., 2019). All types of tissue loss are progressive, differing with species and region, and, in some instances, SCTLD appears transmissible, indicating an infectious etiology (Aeby et al., 2019).

No systematic descriptions of SCTLD exist at the gross or the microscopic level. Such information might shed light on mechanisms or causes of disease, particularly in poorly understood animals such as corals (Work and Meteyer, 2014). Moreover, inferring the etiology of coral disease based solely on gross lesions might be misleading (Work and Aeby, 2006), particularly because TLDs might have multiple manifestations at the cellular level (Work et al., 2012). Our objective here was to systematically describe pathology of SCTLD at the gross and microscopic levels in eight coral species sampled during 2016–2018.

MATERIALS AND METHODS

Study Sites

Tissue samples were collected from eight coral species (*Colpophyllia natans*, *Dendrogyra cylindrus*, *Diploria labyrinthiformis*, *Meandrina meandrites*, *Montastraea cavernosa*, *Orbicella faveolata*, *Pseudodiploria strigosa*, and *Siderastrea siderea*) from 13 sites at which SCTLD was epidemic or endemic (Rosales et al., 2020), ranging from Broward County southward along the Florida Reef Tract to the Lower Florida Keys. Reference samples from apparently healthy corals in regions without SCTLD at the time were collected at two timepoints: in April 2017 from the northernmost portion of the Florida Reef Tract from a site in Martin County and two sites in the Middle Keys, and in May-June 2018 from three sites in the Lower Keys, offshore of Key West. Sites spanned southeast Florida, offshore patch and fore reefs, and midchannel patch reefs in the Florida Keys (**Figure 1**). In 2017 and 2018, unaffected reference sample sites were distant from the SCTLD epidemic boundary but have since been affected.

Coral Sample Collection

Collection methods followed established protocols (Woodley et al., 2008). Samplers measured colony dimensions and recorded whether colonies were diseased or apparently healthy (i.e.,

[1] https://floridadep.gov/sites/default/files/CRCP_Strategic_Plan_2011-2016.pdf

[2] https://floridadep.gov/rcp/coral/content/stony-coral-tissue-loss-disease-response

[3] https://nmsfloridakeys.blob.core.windows.net/floridakeys-prod/media/docs/20181002-stony-coral-tissue-loss-disease-case-definition.pdf

[4] http://www.agrra.org/coral-disease-outbreak/

[5] http://www.thebahamasweekly.com/uploads/21/SCTLD-report-for-Grand-Bahama-3-20_compressed.pdf

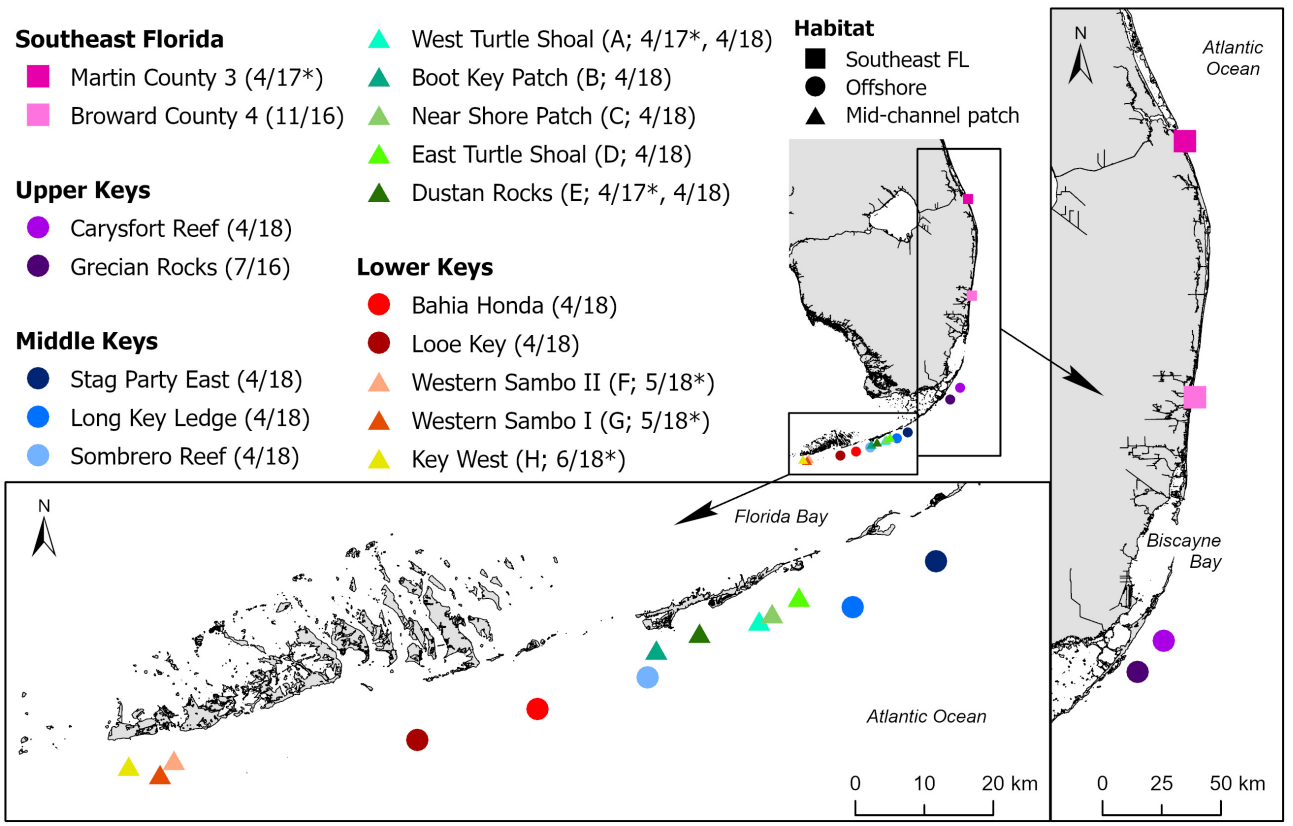

FIGURE 1 | Sites along the Florida Reef Tract at which corals were sampled for stony coral tissue loss disease (SCTLD) histological analysis. Sites are in four regions (Southeast Florida [SE FL] and the Upper, Middle, and Lower Keys) and three general reef habitats (SE FL, offshore, and mid-channel patch). Project site codes = A–H used in **Table 1**, sampling dates = MM/YY, * = site sampled before the arrival of SCTLD.

those showing no evidence of tissue loss or discoloration) before sampling and photographing the whole colony and areas most suitable for a biopsy. A biopsy consisted of a circular core of tissue and skeleton collected using a 25.4-mm-diameter sterilized stainless-steel corer–punch hammered into a colony until it reached a depth sufficient to obtain an ample sample, which varied with species. Individual reference sample tissue cores were collected from apparently healthy colonies (HH [histology healthy]) with no evidence of tissue loss or discoloration either at reference sites without SCTLD or from sites with SCTLD. For each diseased colony, one tissue core was collected from an apparently unaffected tissue area (HU [histology unaffected]), and a second core was taken from the margin between intact tissue and bare skeleton (HD [histology diseased]) (**Table 1**). Apparently healthy corals were always sampled before diseased corals at sites with SCTLD, and a new pair of disposable nitrile gloves was worn for sampling each colony. After collection at each site, a photograph was taken of each biopsy core sample and postbiopsy area on the colony, and each core was placed into its own labeled Whirl-Pak sample bag and taken to the boat for further processing.

On board, sterile bone cutters were used to clip off a small representative portion of each core to be fixed for transmission electron microscopy (TEM). Samples were fixed for histology or TEM immediately after the dive, conditions permitting, or stored in a cooler filled with seawater at ambient temperature (and held in the shade) for transport to the laboratory (and then fixed within < 6 h from collection). To minimize cross contamination between sites during sampling, nitrile gloves were discarded, and all collection equipment sterilized on board in a 5–10% solution of sodium hypochlorite for 20 min.

Samples for histology were preserved in a solution of 1 part Z-Fix (zinc formalin; Z-Fix concentrate [18.5% formaldehyde; Anatech Ltd., Battle Creek, Michigan]) mixed with 4 parts 0.2 μm–filtered natural seawater (or 35 salinity artificial seawater). Samples for TEM were fixed at 4°C with Trump's fixative (4% formaldehyde, 1% glutaraldehyde, 50 mM NaH_2PO_4, pH 7.2; McDowell and Trump, 1976). All processing for histology and TEM was done at the Florida Fish and Wildlife Conservation Commission's (FWC) Fish and Wildlife Research Institute (FWRI), St. Petersburg, FL, United States.

Histopathology

Before histopathology, samples were photographed close up using a digital camera fitted with a macro lens (Nikon, Tokyo). Samples with grossly visible lesions were further examined

TABLE 1 | Coral species and numbers of samples[a] evaluated by histopathological analyses.

Location	Collected	Species	HD	HU	HH	Total
SCTLD sites[b]						
Grecian Rocks	21 Jul 16	*Colpophyllia natans*	3 (2)[c]	3 (1)	1 (0)	7
		Diploria labyrinthiformis	2 (2)	2 (1)	1 (1)	5
		Montastraea cavernosa	3 (3)	3 (0)	1 (0)	7
		Siderastrea siderea	3 (3)	3 (2)	1 (1)	7
Broward County 4	19 Nov 16	*Montastraea cavernosa*	10 (10)	10 (1)	5 (0)	25
		Orbicella faveolata	3 (3)	3 (0)	3 (1)	9
		Siderastrea siderea	3 (3)	3 (0)	3 (1)	9
Sites A–E	9–27 Apr 18	*Colpophyllia natans*	10 (7, 1NA[d])	10 (0, 2NA)	4 (0)	24
		Montastraea cavernosa	10 (10)	10 (1)	5 (1[e])	25
		Orbicella faveolata	10 (7)	10 (1, 1NA)	5 (1)	25
		Pseudodiploria strigosa	10 (7, 2NA)	10 (0)	5 (0)	25
		Siderastrea siderea	10 (6, 1NA)	10 (2)	5 (0)	25
Looe Key	19 Apr 18	*Meandrina meandrites*	5 (5)	5 (0)	3 (0, 1NA)	13
Keys offshore[f]	17–19 Apr 18	*Dendrogyra cylindrus*	6 (3, 2NA)	0	0	6
		Total	88 (71, 6NA)	82 (9, 3NA)	42 (5, 1[e], 1NA)	212
Reference sites						
Martin County 3	25 Apr 17	*Montastraea cavernosa*			5 (0)	5
Site A	26 Apr 17	*Montastraea cavernosa*			2 (0)	2
Site E	27 Apr 17	*Montastraea cavernosa*			3 (1[e])	3
Sites F–G	8 May 18	*Colpophyllia natans*			6 (0)	6
		Montastraea cavernosa			6 (0)	6
		Orbicella faveolata			6 (0)	6
		Pseudodiploria strigosa			6 (0)	6
		Siderastrea siderea			5 (0)	5
Site H	5 Jun 18	*Colpophyllia natans*			3 (0)	3
		Montastraea cavernosa			3 (0)	3
		Orbicella faveolata			3 (0)	3
		Pseudodiploria strigosa			3 (0)	3
		Total			51 (1[e])	51

[a] *Samples are grossly separated by three types: (1) lesioned area at the healthy tissue/tissue-loss margin (HD [histology disease]); (2) unaffected area of the same colony (HU [histology unaffected]); and (3) apparently healthy colony (HH [histology healthy]).*
[b] *Site information is shown in* ***Figure 1****.*
[c] *Numbers with lytic necrosis lesions shown in parentheses.*
[d] *NA = section not suitable for evaluation; deducted from number of samples evaluated.*
[e] *Possible early LN lesion.*
[f] *Opportunistic samples collected from Carysfort Reef, Stag Party East, Long Key Ledge, Sombrero Reef, Bahia Honda, and Looe Key (****Figure 1****).*

under higher magnification with a dissecting microscope attached to an Olympus DP71 digital camera (Tokyo) and photomicrographs were taken.

For ease of orientation and integrity, and to minimize loss of any surface microorganisms after the skeleton had been removed following decalcification, all HD samples were enrobed with 1.5% agarose in a heated vacuum oven (60°C) at 22 mm Hg (Jones and Calabresi, 2007) (HU and HH samples were not enrobed with agarose but otherwise were processed as for HD samples), followed by decalcification with 10% ethylenediaminetetraacetic acid (EDTA-$Na_2{\cdot}2H_2O$, MW = 372.1; Fisher Scientific, Waltham, Pennsylvania) adjusted to pH 6.8–7.2 with NaOH (approximately 9 g per L of solution) on a shaker table (Price and Peters, 2018). Tissue enrobed in agarose was cut with a razor blade to expose the aboral (bottom) side facing the skeletal tissue opening, allowing contact with the EDTA solution. The EDTA solution was changed every 48–72 h until no resistance was felt in placing a razor blade into the tissue. Decalcification took 14–60 days depending on the size (depth of the skeleton) of each sample and longer if the tissue was enrobed. Decalcified tissue samples were then processed for routine histology.

For histology, tissues were trimmed sagittally (perpendicular to the polyp mouth) and radially (parallel to the polyp mouth), embedded in paraffin (Paraplast Plus, Fisher Scientific, Waltham, Pennsylvania) or glycol methacrylate plastic resin (JB-4; Electron Microscopy Sciences, Hatfield, Pennsylvania), sectioned at 4.0 μm, and stained with Mayer's hematoxylin and eosin (H and E) or periodic acid–Schiff–metanil yellow (PAS-MY for JB-4 or PAS-hematoxylin for paraffin). Additional stains were used as needed to confirm various microscopic findings including alcian blue (for mucopolysaccharides), Brown and Brenn

Gram (bacteria), Feulgen (DNA), Fontana-Masson (FM) silver (melanin), Grocott's methenamine-silver nitrate (GMS) (fungi), May-Grünwald Giemsa (protozoa), Macchiavello (chlamydia), methyl green pyronin (MGP) (DNA), Perl's Prussian blue (iron), and thionin (DNA) (Luna, 1968; Quintero-Hunter et al., 1991; Price and Peters, 2018; FWC-FWRI unpubl. data). Slides were examined with an Olympus BX51 light microscope equipped with an Olympus DP71 digital camera (Olympus Inc., Tokyo).

Transmission Electron Microscopy

After histological evaluation, samples showing specific areas of interest were chosen for TEM study. Samples were decalcified with 10% EDTA solution for 8 days without agarose enrobing, cut into an appropriate size (approximately 1 × 1 × 1 mm), followed by postfixation with 1% osmium tetroxide in 1.25% $NaHCO_3$ buffer, pH 7.2, for 1 h at room temperature. Tissue samples were washed in Nanopure water three times for 5 min each and then dehydrated in a graded series of ethanol and embedded in Spurr epoxy resin (Sigma-Aldrich, St. Louis, Missouri). The epoxy block was sectioned for semithin sections with a Leica EM UC6 ultramicrotome (Leica Microsystems, Vienna) attached with a glass knife, at 1-μm thickness, adhered onto a glass slide, stained with toluidine blue, mounted with a cover glass, and examined under light microscopy for preparation quality and tissue condition. Ultrathin sections (90 nm) were cut with a diamond knife on the ultramicrotome and placed on copper grids. The sections were then stained with 2% uranyl acetate in 50% ethanol and lead citrate (Reynolds, 1963) and examined with a Jeol JEM-1400 transmission electron microscope (JEOL, Tokyo) equipped with a digital photomicrograph ORIUS^{TM} SC1000 CCD camera (GATAN Inc., Pleasanton, California) in TEM brightfield mode at 80 kV.

RESULTS

A total of 263 samples, comprising eight species of corals from 17 sites (13 diseased and 6 reference sites [of which 2 were diseased the following year, sites A and E, and were re-sampled as diseased sites]) (**Figure 1**), were processed from 88 diseased colonies comprising 88 tissue-loss lesions (HD) and 82 grossly unaffected tissues (HU) from the same diseased colonies (except for *Dendrogyra cylindrus* which had no HU collected). An additional 42 unaffected tissues from apparently healthy (HH) colonies were collected in the same SCTLD-affected sites. Finally, unaffected tissues from 51 apparently healthy (HH) reference colonies were taken in SCTLD-free sites (**Table 1**).

Gross Description

Grossly, SCTLD comprised varying shapes and sizes of amorphous distinct areas of tissue loss revealing (1) wide areas (∼50 mm or more width) of recent necrosis indicated by intact

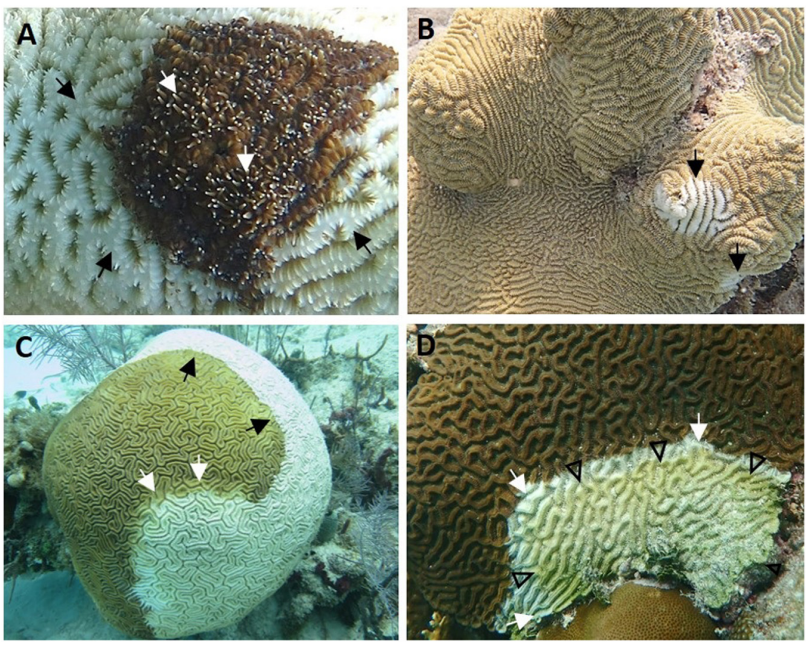

FIGURE 2 | Gross acute to subacute lesions of stony coral tissue loss disease. **(A)** *Dendrogyra cylindrus* with acute tissue loss (black arrows). Note distinct area of bare white skeleton surrounding intact tissue, with tentacles extended (white arrows) from some polyps. **(B)** *Meandrina meandrites* with multifocal acute tissue loss. Note distinct areas of bare white skeleton on edge and center of colony (arrows). **(C)** *Diploria labyrinthiformis* with diffuse acute tissue loss. Note distinct area of bare white skeleton apposed to intact tissue (black arrows) with intermittent bands of pallor at lesion edge (white arrows). **(D)** *Colpophyllia natans* with focal subacute tissue loss. Note distinct domed area of bare white skeleton apposed to intact tissue (white arrows) arising from colony edge (bottom) followed by an area of exposed bare skeleton covered in turf algae and debris (arrowheads). **(A)** Stag Party East, April 2018; **(B)** Looe Key, April 2018; **(C)** Grecian Rocks, July 2016; **(D)** Dustan Rocks, April 2018. Photos: **(A)** Karen Neely; **(B)** Tiffany Boisvert; **(C)** Vanessa Brinkhuis; **(D)** Brian Reckenbeil.

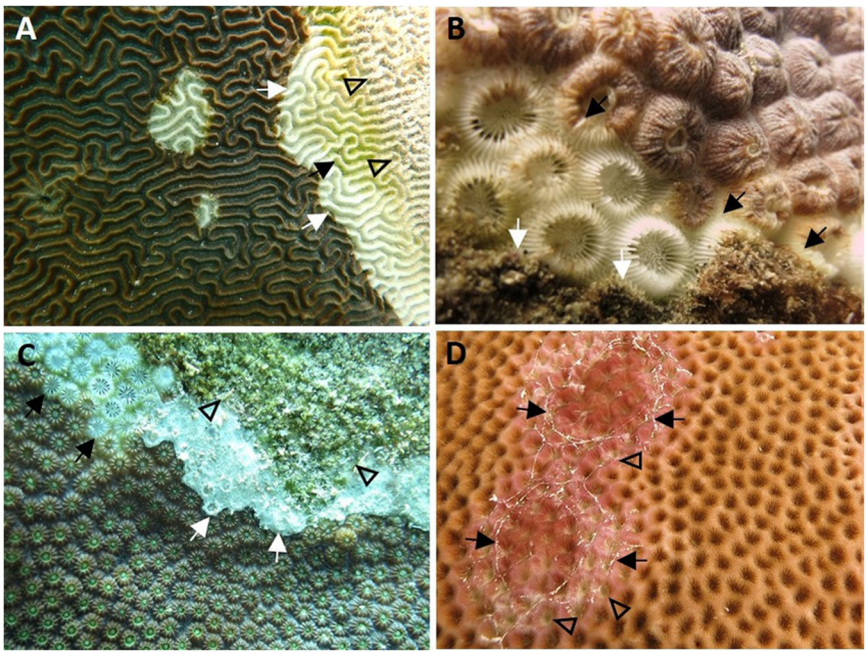

FIGURE 3 | Gross acute to chronic lesions and discoloration in stony coral tissue loss disease. **(A)** *Pseudodiploria strigosa* with multifocal acute to subacute tissue loss. Note exposed skeleton bereft of tissues partly overgrown by green turf algae (black arrow) with area further from the tissue loss margin (white arrows) covered with particulate matter (arrowheads). **(B)** *Montastraea cavernosa* with subacute to chronic tissue loss. Note distinct to indistinct band of bare white skeleton behind active disease margin (black arrows) and followed by turf overgrowth (white arrows). **(C)** *Orbicella faveolata* with chronic tissue loss. Note area of tissue loss revealing bare white skeleton (black arrows) and what appears to be a white biofilm at the tissue-loss interface (white arrows), both followed by turf overgrowth (arrowheads). **(D)** *Siderastrea siderea* with multifocal to diffuse subacute to chronic tissue loss and pinkish discoloration, with outer edges of chronic lesions covered with mucus strands (arrows). Note tissue-loss areas (arrowheads) radiating from the polyps' oral regions and surrounding septa between adjacent polyps. **(A)** Near Shore Patch, April 2018; **(B,C)** Broward County, November 2016; **(D)** Grecian Rocks, July 2016. Photos: **(A)** Brian Reckenbeil; **(B,D)** Lindsay Huebner; **(C)** Vanessa Brinkhuis.

bare white skeleton and absent turf algal overgrowth (acute tissue loss, **Figures 2A–C**), (2) less wide (∼10–50 mm width) but still prominent areas of recent necrosis (subacute tissue loss, **Figures 2D**, **3A,B**), or (3) narrow (∼10 mm or less width) to almost unnoticeable areas of recent necrosis apposed to skeleton overgrown with turf algae (chronic tissue loss, **Figure 3C**). Stony coral tissue loss disease in *S. siderea* appeared to present differently, with multifocal pinkish discoloration around the polyps and the surrounding septa, frequently with mucus strands present on the outer areas of the lesion (**Figure 3D**). Location of tissue loss did not have any pattern; lesions appeared near the bottom, top, or edges of colonies regardless of species affected.

At the macroscopic level, the lesions differed in appearance depending on the anatomy of the affected species. In general, however, there was a distinct margin between healthy tissue and bare skeleton. Brain corals (*C. natans*, *Diploria labyrinthiformis*, and *P. strigosa,* family Faviidae) showed lesion margins that could traverse adjacent septa (**Figure 4A**). In *M. cavernosa* and *O. faveolata* (families Montastraeidae and Merulinidae, respectively), tissue loss appeared to progress along the top of the septa, where the surface tissue is thin, allowing spreading across neighboring septa around the polyp while progressing across to a different polyp (**Figure 4B**). In pillar or maze corals (*Dendrogyra cylindrus* and *Meandrina meandrites*, family Meandrinidae), borders of areas of tissue loss were more undulating (**Figure 4C**). In *S. siderea*, pinkish discoloration associated with tissue loss appeared around the oral region and surrounding septa (**Figure 4D**).

Histopathological and Ultrastructural Description

The low-magnification overview showed that lytic necrosis (LN)[6] first affected the basal body wall (BBW) gastrodermis **(Figure 5A)** and progressed toward the surface body wall (SBW) (polyps and coenenchyme), presenting grossly as tissue loss. In advanced lesions, in *P. strigosa*, for example, necrosis appeared to advance across the full thickness of the SBW and BBW, forming a transitional boundary between degraded areas and intact tissue (**Figure 5B**).

At the cellular level, putative early lesions of SCTLD appeared to start with zooxanthellae in the otherwise intact BBW gastrodermis. In some apparently healthy corals from healthy reference (**Figures 6A,B,D**) or SCTLD-affected

[6]Lytic necrosis as used in this article is similar to liquefactive necrosis as that is defined in the general pathology nomenclature (i.e., focal, multifocal, or diffuse area of microscopic tissue necrosis accompanied by surrounding cell lysis). To clearly avoid misunderstanding of the definition of liquefactive necrosis because of the cytological and anatomical differences between vertebrates and invertebrates, we decided to use the term lytic necrosis herein.

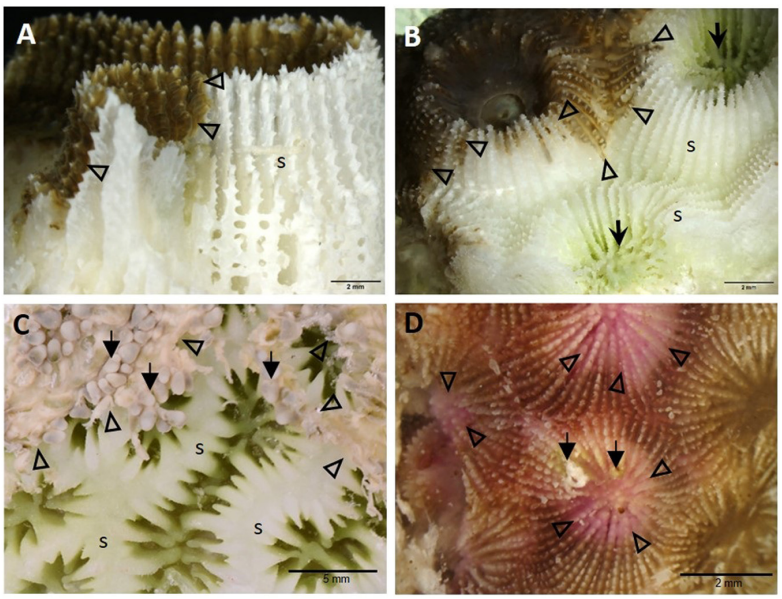

FIGURE 4 | High-magnification gross macrophotographs of fixed core samples showing different anatomical examples of demarcation borders between tissue-loss margins and apparently healthy surface areas in various species. **(A)** *Pseudodiploria strigosa* showing exposed white skeleton adjacent to active disease margin (arrowheads) along the septum. **(B)** *Montastraea cavernosa* showing the multifocal progression of tissue loss (arrowheads) along the septa of two adjacent polyps. Note green algal coloration (arrows) in chronically exposed bare skeleton around the oral regions. **(C)** *Dendrogyra cylindrus* showing the progression of the tissue-loss margins (arrowheads) around the polyps, with some tentacles still partly intact (arrows), exposing the skeletal ridges. **(D)** *Siderastrea siderea* with pinkish discoloration of tissue loss areas around the polyp oral cavities and septa, showing tissue-loss margins (arrowheads) and overgrowth of algae (arrows). **(A)** Near Shore Patch, April 2018; **(B,D)** Broward County, November 2016; **(C)** Long Key Ledge, April 2018. s = skeleton.

(**Figure 6C**) sites, zooxanthellae were necrotic or swollen, with intracytoplasmic vacuolation of the gastrodermis, mesogleal edema, and vacuolation of the calicodermis (**Figure 6A**), with exocytosis of zooxanthellae (**Figure 6B**), and pyknosis of the calicodermis (**Figures 6B,C**). In *Montastraea cavernosa*, individual or clusters of crystalline inclusion bodies (CIBs; details described below) were seen adjacent to zooxanthellae or vacuolated areas in the gastrodermis (**Figures 6A-C**). At the tissue level, putative early-stage lesions of SCTLD appear to start in the BBW of the septum or coenenchyme (**Figures 6D-F**), with early foci of initiating LN seen along the gastrodermis of the BBW (**Figure 6D**), advancing with a cleft forming between the BBW gastrodermis and the calicodermis (**Figure 6E**) and progressing to multifocal BBW LN with necrotic tissue sloughing into the gastrovascular canal (GVC) (**Figure 6F**).

Presumptively in parallel with pathology in BBW zooxanthellae, cellular changes in the SBW were seen, with zooxanthellae initially affected, followed by SBW gastrodermal pathology. Zooxanthellae exhibited necrosis with dilation of symbiosomes, and gastrodermis had intracytoplasmic vacuolation (**Figure 7A**), with zooxanthellae showing accumulation of intracytoplasmic refractile granules, hypopigmentation, deformation, or fragmentation (**Figures 7B–F**). The lesion seemed to progress to enlargement of the symbiosome surrounding zooxanthellae (**Figures 7C–D**), some of which manifested coagulation necrosis of individual zooxanthellae (**Figure 7C**) and coalescence of symbiosomes (**Figures 7A,D–F**). In advanced lesions, there was diffuse LN of the gastrodermis of the SBW and BBW (**Figure 7E**), with necrotic zooxanthellae that occasionally stained positive (presumptive melanin, dark brown to black) with FM (**Figures 7E,F**).

On TEM in *M. cavernosa*, degraded coral gastrodermal cells were seen, with vacuolated cytoplasm filled with debris, phagosomes, degenerating nuclei, shrunken zooxanthellae with a loss of symbiosome membranes, and a general collapse of the symbiont–host cell integrity (**Figure 8A**). Mucocytes were in somewhat better condition (**Figure 8A**). Zooxanthellae showed varying degrees of nuclear fragmentation and degeneration with the formation of condensed peripheral chromatin (**Figures 8B–D**), degrading chloroplasts with loss of thylakoid structure (**Figure 8C**), and enlarged accumulation bodies with cellular debris (**Figure 8D**).

Advancement of LN into the SBW was observed initially in the gastrodermis. Distention of the symbiosome surrounding the zooxanthellae expanded beyond the basement membrane of the gastrodermis and into the mesoglea, leading to its fragmentation (**Figures 9A,B**). This progressed to full-scale gastrodermal necrosis, with release of cell debris and zooxanthellae into the GVCs (**Figures 9C,D**), mesogleal vacuolation and necrosis (**Figure 9**), and progression of vacuolation beyond the epidermal basement membrane (**Figure 9C**). Lesion advancement was followed by collapse of the mesoglea and sloughing of the epidermis (**Figure 9D**).

In *Meandrina meandrites*, *Montastraea cavernosa*, *P. strigosa*, and *O. faveolata*, initiation of necrosis of the gastrodermis of the SBW often occurred near areas of advanced necrosis of the

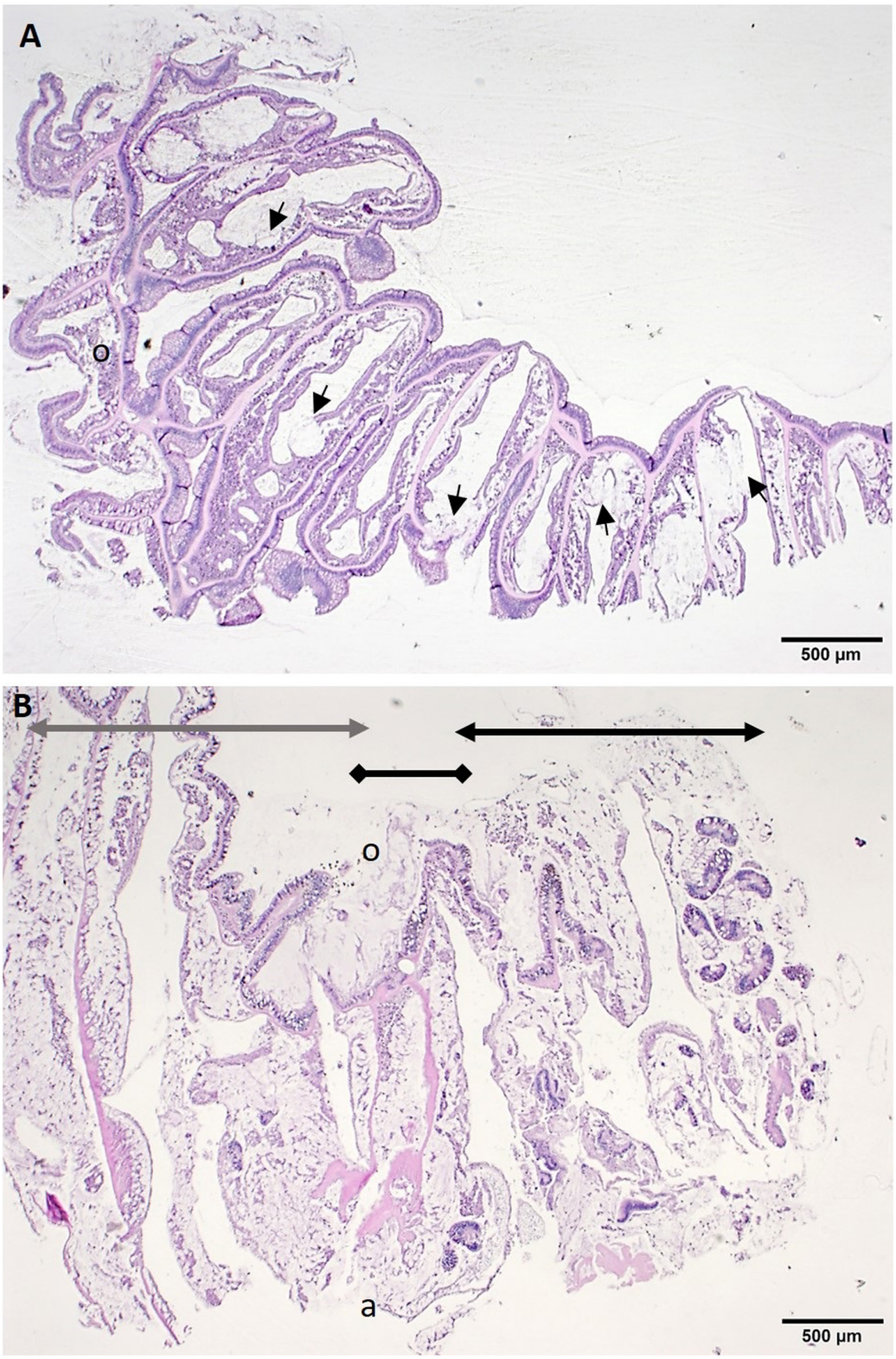

FIGURE 5 | Low magnification of histological sections of tissue-loss area. **(A)** Radial section through half a polyp along the septa of *Montastraea cavernosa* showing lesions adjacent to the skeleton in the basal body wall (BBW). Note foci of lytic necrosis (LN) in the BBW (arrows). **(B)** Sagittal section through tissue-loss boundary area in *Pseudodiploria strigosa* showing extensive coagulative necrosis including sloughed surface epidermis (black double-arrow line), lesion margin (black double-diamond line) and apparently healthy tissue zone (gray double-arrow line). H and E, o = oral region, a = aboral region.

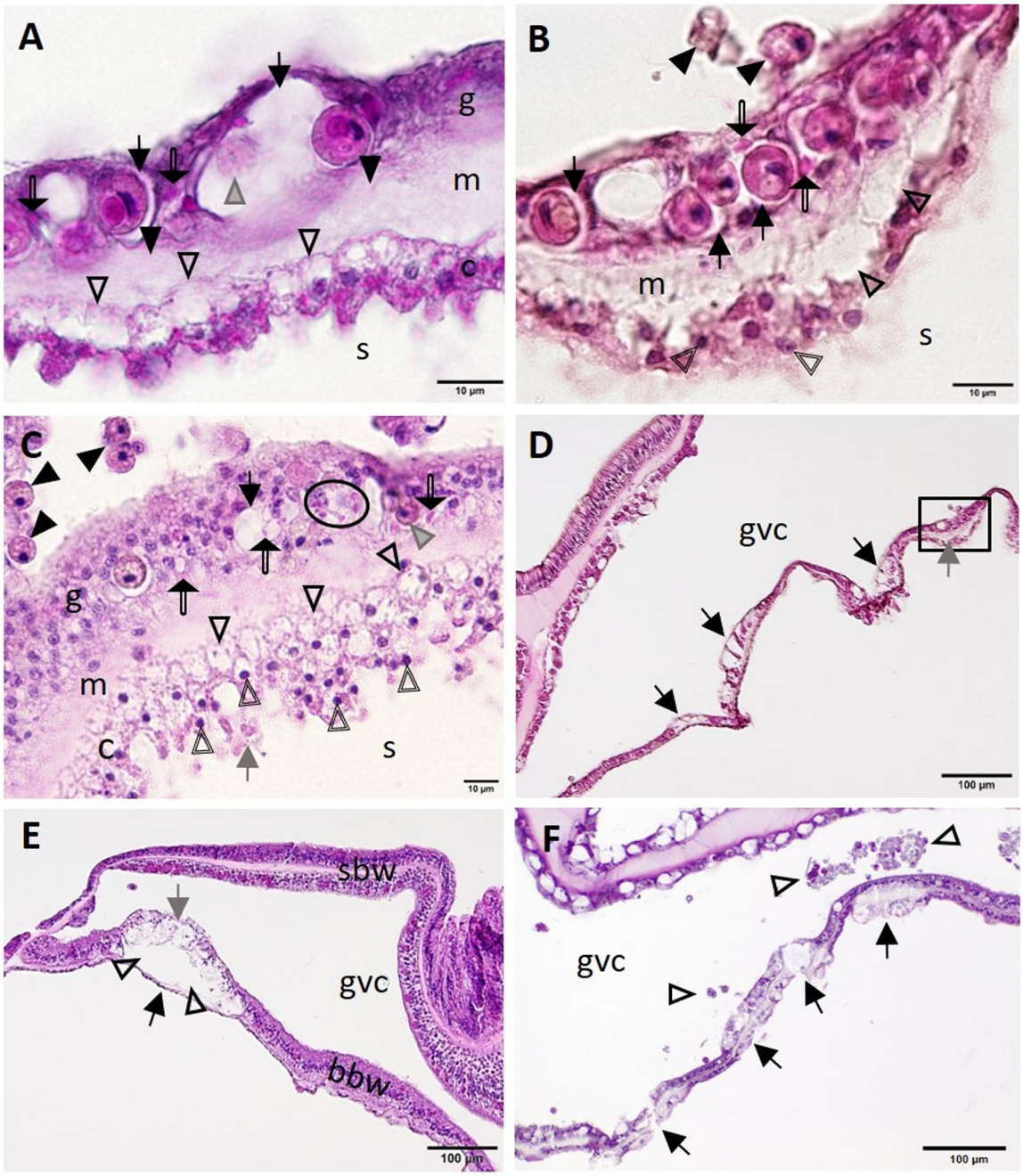

FIGURE 6 | Putative initiation of basal body wall (BBW) lesion formation in *Montastraea cavernosa* **(A–D,F)** and early lytic necrosis (LN) lesion in *Dendrogyra cylindrus* **(E)**. **(A)** Initial mesogleal swelling and edema (closed arrowheads), swelling of zooxanthella symbiosomes (arrows), necrosis of a zooxanthella (gray arrowhead), crystalline inclusion bodies (CIBs) (double-line arrows), and hypertrophic calicodermal cells with marked cytoplasmic vacuolation (open arrowheads). **(B)** High magnification of inset area marked in **(D)** shows mesogleal edema with marked vacuolation (open arrowheads), swelling of zooxanthellae symbiosomes (arrows), CIBs (double-line arrows), exocytosis of zooxanthellae (closed arrowheads), and pyknotic calicoblasts (double-line arrowheads). **(C)** Putative calicodermal lesion initiation showing high density of pyknotic nuclei (double-line arrowheads; normal nucleus = gray arrow) and markedly vacuolated calicodermis (open arrowheads) adjacent to skeleton. Note exocytosis of vacuolated zooxanthellae (closed arrowheads), gastrodermal vacuolation (black arrow), necrotic zooxanthella (gray arrowhead), and individual (double-line arrows) or cluster of CIBs (oval) in gastrodermis. **(D)** Four focal areas in the BBW showing gastrodermal vacuolation (arrows) and mesogleal edema (gray arrow) (inset, see **B**). **(E)** Localized LN of the BBW leading to cleft formation (arrowheads) between apparently intact calicodermis (black arrow) and necrotic vacuolated gastrodermis (gray arrow). Note the intact surface body wall (SBW). **(F)** Multifocal LN in the BBW (arrows) with necrotic tissue and zooxanthellae (arrowheads) sloughed into the gastrovascular canal (GVC). **(A,B,D)** Apparently healthy reference colony, Dustan Rocks, April 2017; **(C)** apparently healthy colony, Near Shore Patch, April 2018; **(E)** diseased colony, Long Key Ledge, April 2018; **(F)** diseased colony, Broward County, November 2016. **(A)** Periodic acid–Schiff (PAS); **(B–F)** Hematoxylin and eosin (H and E). bbw, basal body wall; c, calicodermis; g, gastrodermis; gvc, gastrovascular canal; m, mesoglea; sbw, surface body wall; s, skeleton.

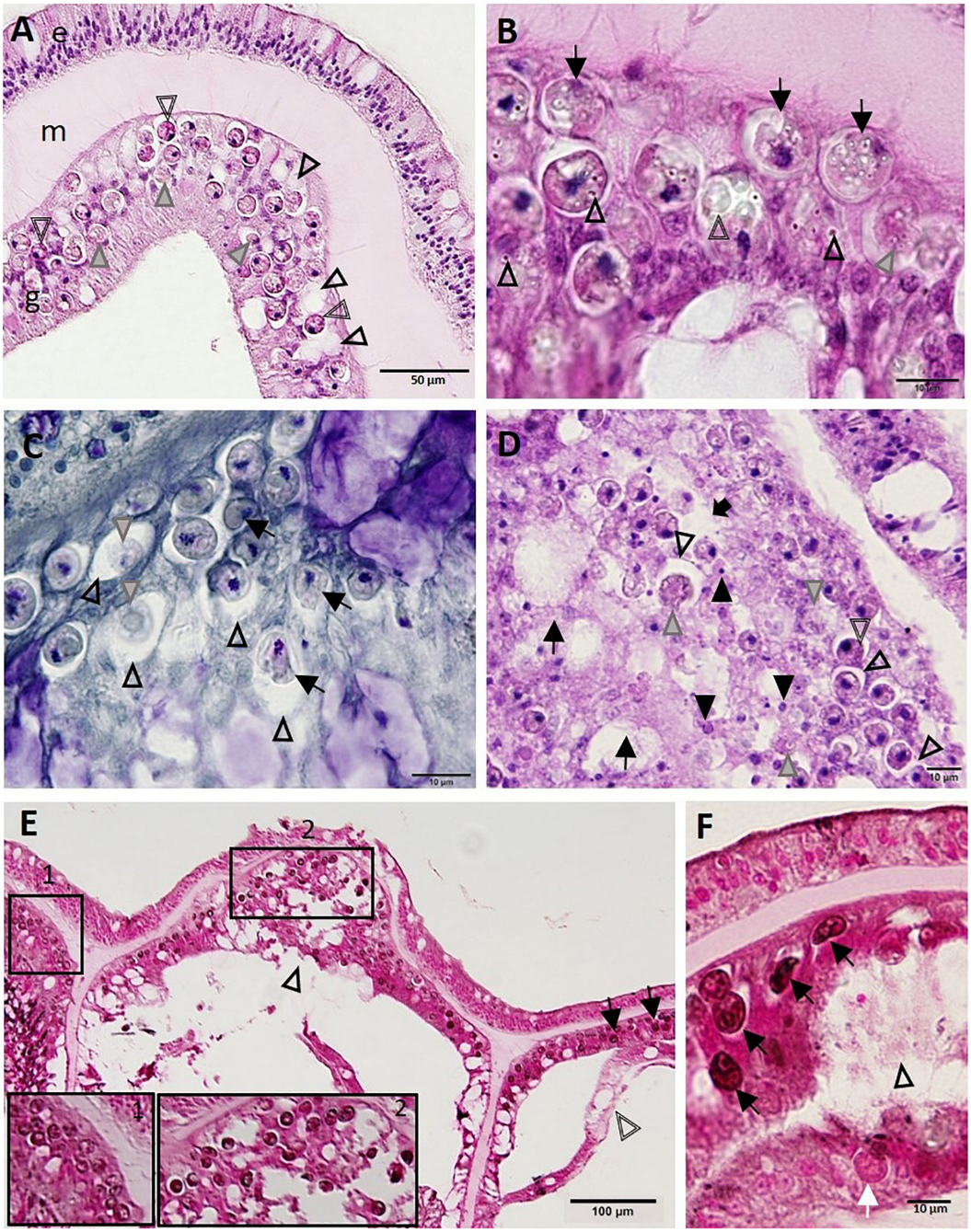

FIGURE 7 | Progressive zooxanthellae pathology in the surface body wall. **(A)** Intact mesoglea and epidermis with initial zooxanthellae pathology in the gastrodermis in *Montastraea cavernosa*. Note necrotic zooxanthellae with dilated symbiosomes (gray arrowheads) and cytoplasmic hypereosinophilia (double-line arrowheads), and coalescing vacuolation of the gastrodermis (arrowheads). **(B)** Gastrodermis of *M. cavernosa* showing deformed zooxanthellae (arrows) with intracytoplasmic refractile vacuoles (arrowheads), hypopigmentation (gray arrowhead), or fragmentation (double-line arrowhead). **(C)** Gastrodermis of *Diploria labyrinthiformis* manifesting zooxanthellae disruption. Note distended symbiosomes (arrowheads) with some zooxanthellae showing deformation (arrows) or coagulation necrosis (gray arrowheads). **(D)** Gastrodermis of *Colpophyllia natans* manifesting multifocal necrosis. Note massive disruption and lytic necrosis (LN) of gastrodermal cells (black arrows) with karyorrhectic and pyknotic nuclei (closed arrowheads), deformed and necrotic zooxanthellae (gray arrowheads), some of which manifest cytoplasmic hypereosinophilia (double-line arrowhead) or dilation of symbiosomes (open arrowheads) that eventually coalesce (black arrow). **(E)** Apparently healthy zooxanthellae (pink-red to light brown) with evident pyrenoids and lack of visible symbiosomes (inset 1) in intact SBW gastrodermis of *M. cavernosa*. Compare to abnormal dark zooxanthellae with no pyrenoids and dilated symbiosomes (inset 2 and arrows) in LN lesion in surface body wall (SBW) gastrodermis showing marked disruption and vacuolation (arrowhead) and adjacent to basal body wall (BBW) LN lesion (double-line arrowhead). **(F)** Gastrodermal LN lesion (arrowhead) in *M. cavernosa* with associated deformed zooxanthellae (black arrows) staining FM-positive (black) compared to a normal (pink-red) zooxanthella (white arrow). **(A,B,D)** Hematoxylin and eosin (H and E); **(C)** Macchiavello; **(E,F)** Fontana-Masson (FM). e, epidermis; g, gastrodermis; m, mesoglea.

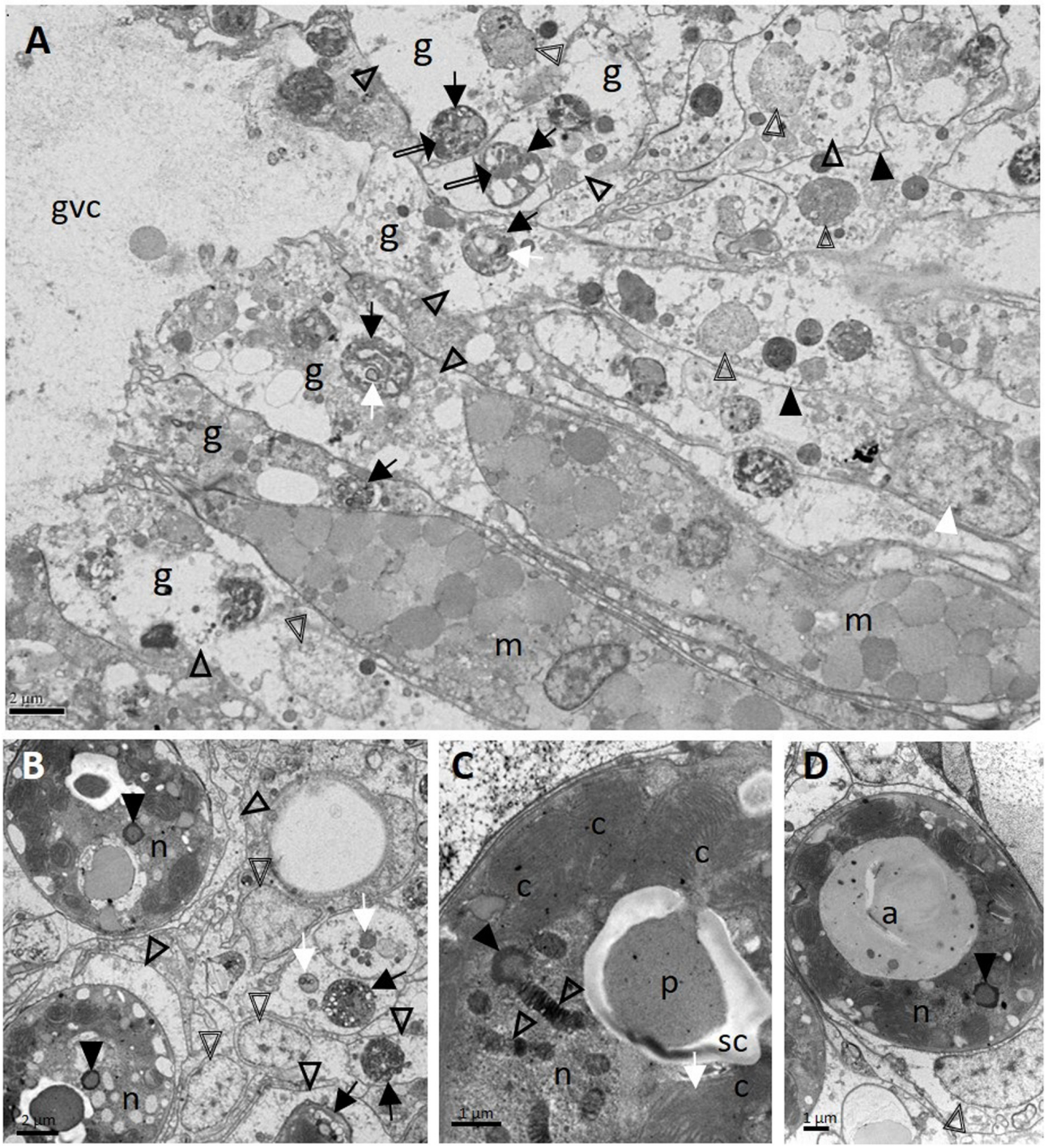

FIGURE 8 | Ultrastructure of *Montastraea cavernosa* surface body wall gastrodermis showing pathology of coral host cells and zooxanthellae. **(A)** Note intact mucocytes adjacent to gastrodermal cells manifesting marked vacuolation with intact cell membranes (closed arrowheads), an intact nucleus (white arrowhead), or degrading nuclei (double-line arrowheads) leading to loss of tissue architecture. Note zooxanthellae ex hospite (arrows) manifesting varying stages of intracytoplasmic vacuolation, some with shrunken pyrenoids (white arrows), dilated symbiosomes with debris (open arrowheads), and different-size clumps of variably electron-dense material (possible lipid) (double-line arrows). **(B)** Zooxanthellae showing degrading nuclei with peripheral chromatin (closed arrowheads), enlarged vacuolar matrices (open arrowheads) filled with debris (white arrows) and at different states of shrinkage (black arrows). Double-line arrowheads point to host-cell nuclei. **(C)** Zooxanthella showing degrading chromatin in permanently condensed chromosomes of nucleus (open arrowheads), formation of condensed peripheral chromatin (closed arrowhead), and a degenerating chloroplast with loss of thylakoid lamellar structure (white arrow). **(D)** Degenerating zooxanthella showing an enlarged accumulation body and nucleus with an area of degrading peripheral chromatin (arrowhead). Note host-cell nucleus (double-line arrowhead) still intact. a, accumulation body; c, chloroplasts; g, gastrodermal cell; gvc, gastrovascular canal; m, mucocytes; n, nucleus; p, pyrenoid; sc, starch cap.

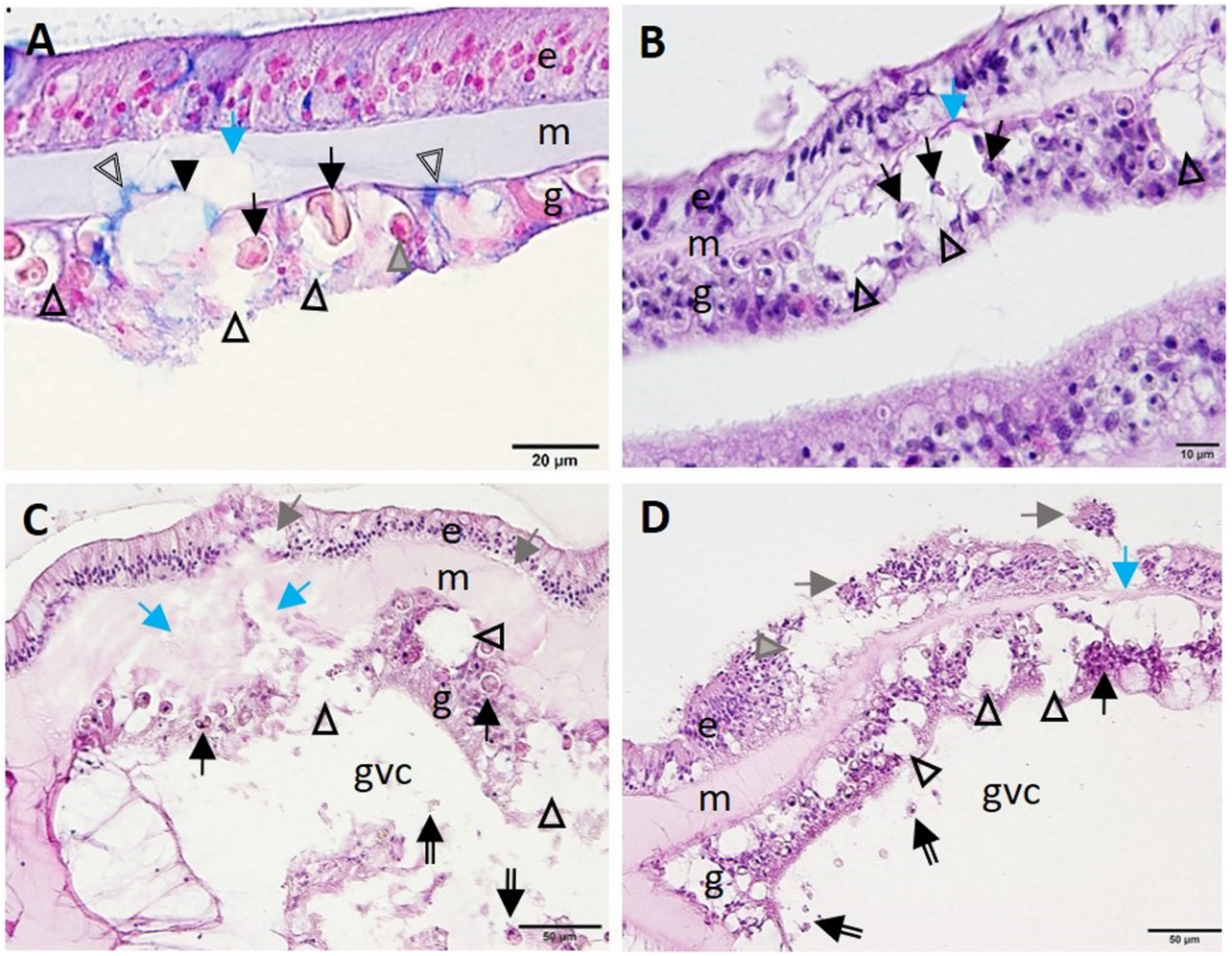

FIGURE 9 | Advance of lytic necrosis (LN) in the surface body wall. **(A)** Gastrodermis of *Montastraea cavernosa* manifesting early-stage LN. Note markedly deformed zooxanthellae (arrows), some of which are shrunken, with hypereosinophilic cytoplasm (gray arrowhead) surrounded by greatly expanded symbiosomes (open arrowheads) disrupting hypertrophic mucocytes (indicated by blue-stained area, double-line arrowheads), the cellular architecture of the gastrodermis (closed arrowhead), and the mesoglea (blue arrow). **(B)** *Meandrina meandrites* manifesting progressive LN in the gastrodermis. Note large coalescing vacuoles disrupting cellular gastrodermal architecture (arrowheads) with necrotic zooxanthellae (black arrows) and collapse of the mesoglea (blue arrow). **(C)** *Montastraea cavernosa* manifesting progressive expansion of LN toward the surface epidermis. Note fragmented and necrotic gastrodermis (arrowheads) with necrotic zooxanthellae (arrows) and fragmented mesoglea (blue arrows) eith cellular debris in the gastrovascular canal (double-line arrows), mesogleal swelling and breached epidermis (gray arrows). **(D)** *Colpophyllia natans* manifesting lesion progression. Note marked vacuolation and disruption of gastrodermal architecture (arrowheads), necrosis (black arrow), cellular debris in the GVC (double-line arrows), collapse of mesoglea (blue arrow), and epidermal sloughing (gray arrows) and vacuolation (gray arrowhead). **(A)** Alcian blue; **(B–D)** hematoxylin and eosin (H and E). e, epidermis; g, gastrodermis; gvc, gastrovascular canal; m, mesoglea.

BBW (**Figure 10**), supporting the hypothesis that lesions start in the BBW and progress to the SBW. Advanced LN lesions in the BBW were associated with initial SBW gastrodermal necrosis (**Figures 10A-C**) and tissue sloughing into the GVC (**Figure 10C**), to mesogleal disruption and gastrodermal atrophy (**Figure 10D**).

End-stage lesions at the tissue level involved SBW epidermal necrosis and sloughing (**Figure 11A**), full thickness necrosis of all tissue layers of areas of the BBW and the SBW with segmental (**Figure 11B**) to diffuse (**Figure 11C**) distribution, necrosis of the mesenterial filaments (**Figures 11D,E**), and necrosis of the tentacular gastrodermis (**Figure 11F**). In *S. siderea*, mesenterial calicoblasts with eosinophilic granules (coral acid–rich proteins, CARPs) were prominent (**Figure 11B**, inset).

Other less consistent findings were seen on histology. Intracytoplasmic polyhedral CIBs (∼1–10 µm in length) were seen mostly in the BBW and, occasionally, SBW gastrodermis of apparently healthy and diseased *M. cavernosa* and *P. strigosa*. These stained positive with PAS (**Figures 12A,B**) and were sometimes associated with LN (**Figure 12B**) or, in *M. cavernosa,* presumptive early-stage lesions (**Figure 6A-C**). Crystalline inclusion bodies stained dark green with toluidine blue (**Figure 12C**) and Feulgen, pale blue with thionin, and black with FM, but negative with GMS, Prussian blue, Macchiavello,

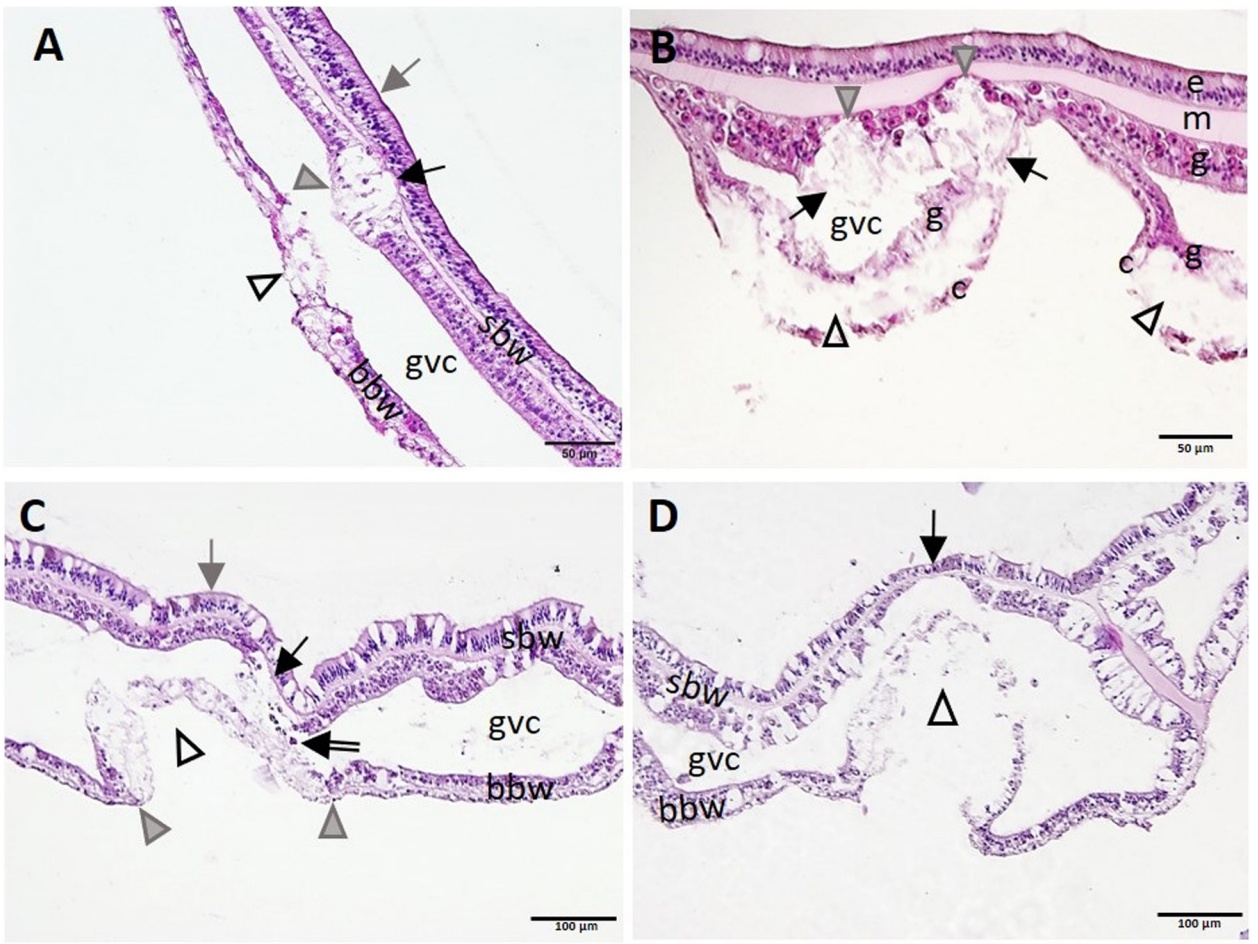

FIGURE 10 | Apparent progression of lytic necrosis (LN) lesions from the basal body wall (BBW) to the surface body wall (SBW). **(A)** *Meandrina meandrites* showing progression of focal LN in the BBW to the adjacent SBW. Note focal areas of full thickness LN of the BBW (open arrowhead), LN of adjacent gastrodermis of SBW (gray arrowhead), and collapse of the mesoglea (black arrow), with epidermis still intact (gray arrow). **(B)** *Montastraea cavernosa* manifesting multifocal LN of the BBW. Note localized areas of cleft formation (open arrowheads) separating necrotic calicodermis and gastrodermis of the BBW, vacuolation and loss of architecture of nearby gastrodermis of the SBW (arrows), with lesion advance toward the mesoglea (gray arrowheads), still with epidermis intact. **(C)** *Pseudodiploria strigosa* manifesting advancing LN of the BBW and progression to the gastrodermal SBW. Note intact SBW epidermis (gray arrow) and diffuse LN of BBW (open arrowhead) distinctly delineated from intact BBW to either side (boundary, gray arrowheads). Note also LN of adjacent gastrodermis of nearby SBW (black arrow) and sloughing of necrotic tissue and zooxanthellae into the GVC (double-line arrow). **(D)** BBW LN in *Orbicella faveolata*. Note same lesion as in **(C)** for BBW (arrowhead), but, in contrast, see localized attenuation and atrophy of nearby gastrodermis of SBW (arrow). Hematoxylin and eosin (H and E). bbw, basal body wall; c, calicodermis; e, epidermis; g, gastrodermis; gvc, gastrovascular canal; m, mesoglea; sbw, surface body wall.

Gram, Giemsa, and MGP. On TEM, CIBs were electron-dense (**Figures 12D,E**), with arrays or a lattice structure of closely packed tubules, with small individual spheres (**Figures 12F,G**) measuring ∼17.6 ± 3.1 (SD) nm diameter (range 14.7–22.2 nm; n = 5, CIBs measured in a grid specimen).

Other structures seen on histology in all species examined included clusters of either coccoidlike [dark blue to mauve in thionin (**Figures 13A,D**) or Giemsa (**Figures 13B,C**)] or coccobacilloidlike (pale to medium magenta in Giemsa, **Figures 13B,C**). Gram-neutral structures often distributed across multiple cells mainly in the gastrodermis of the BBW or SBW but occasionally in LN lesions (**Figure 13D**). Various organisms were seen in healthy and diseased corals but were considered incidental findings because of their consistent lack of association with cell pathology. These included trichodinid ciliates on diseased and healthy *O. faveolata, S. siderea*, *C. natans*, *P. strigosa*, and *D. cylindrus* (**Figure 13E**), unidentified ciliates infesting the deeper GVCs in some diseased corals of all species except *Meandrina meandrites*, and *Halofolliculina* sp. (confirmed with dissecting microscope) on recently denuded skeletons of *O. faveolata*, *Montastraea cavernosa*, *D. cylindrus*, *P. strigosa*, and *S. siderea*. Apicomplexan sporozoites were observed in the actinopharyngeal epithelium of *M. cavernosa* (**Figure 13F**), and apicomplexan oocysts and sporozoites of *Gemmocystis cylindrus* were seen in the mesentery gastrodermis of *D. cylindrus.* Finally, endolithic algae and fungal hyphae (PAS-positive or GMS-positive) were commonly present in the skeleton of all

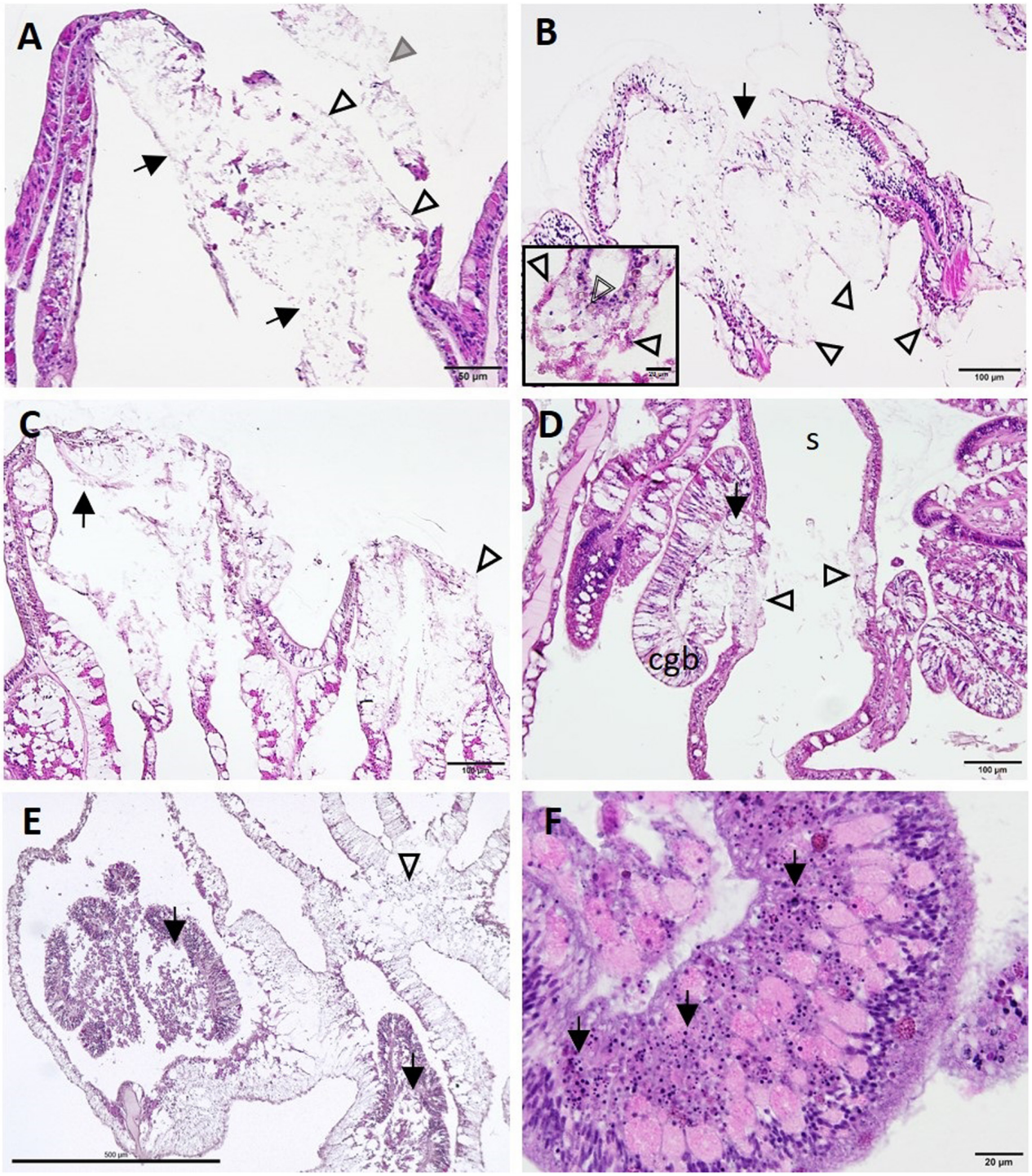

FIGURE 11 | Lesion progression toward advanced tissue loss **(A–C)** and spread to various tissue compartments **(D–F)**. *(A)* Advanced lytic necrosis (LN) in the basal body wall (BBW) (arrows) and surface body wall (SBW) (open arrowheads) of *Dendrogyra cylindrus* at the tissue-loss margin. Note almost complete LN of the BBW and SBW and sloughing of necrotic SBW (gray arrowhead). **(B)** Advanced LN at the tissue-loss margin in *Siderastrea siderea*. Note segmental necrosis of the BBW and SBW (arrow) and remnant calicodermal layer (arrowheads). Inset high magnification showing deeper mesentery with eosinophilic calicoblasts manifesting CARPs (arrowheads) and a brown necrotic zooxanthella (double-line arrowhead). **(C)** Severe LN in *Orbicella faveolata* at the tissue loss margin (arrow). Note more diffuse segmental necrosis (arrowhead) compared with **(B)**. **(D)** LN in the mesentery and cnidoglandular band (CGB) adjacent to LN in the BBW of *Montastraea cavernosa*. Note CGB vacuolation and necrosis (arrow) and BBW LN on either side of the skeleton (arrowheads). **(E)** Deeper in the polyp in *O. faveolata*, note diffuse coagulation necrosis of the mesenterial filaments (arrows) and the BBW (arrowhead). **(F)** Diffuse necrosis (karyorrhexis) of the tentacular gastrodermis (arrows) in *D. cylindrus* (JB-4 medium). Hematoxylin and eosin (H and E), cgb, cnidoglandular band; s, skeleton.

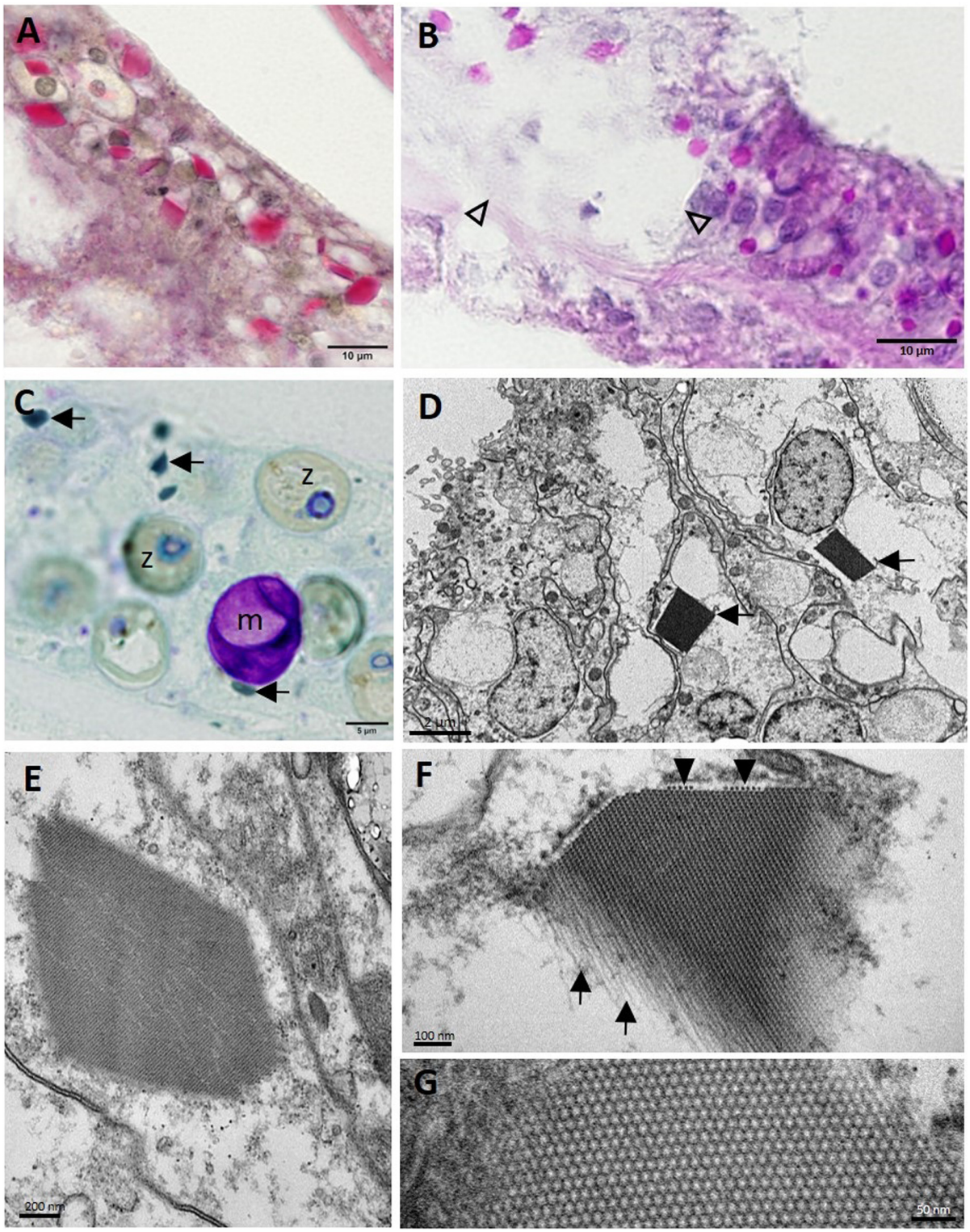

FIGURE 12 | Crystalline inclusion bodies (CIBs) in the basal body wall gastrodermis in *Montastraea cavernosa*. **(A)** Staining periodic acid–Schiff **(**PAS)-positive (red). **(B)** Staining PAS-positive (pink-red) in LN lesion (arrowheads) and adjacent gastrodermal tissue. **(C)** Dark green−staining CIBs (arrows). **(D)** Two CIBs (arrows) each in the cytoplasm of a degenerating mucocyte. **(E)** CIB showing striated appearance. **(F)** High magnification of a CIB showing the filamentous tubular appearance (arrows) and cross section of tubules (arrowheads) that form the striations seen in **(E)**. **(G)** High magnification of CIB showing the lattice pattern of the individual tubes or filaments in cross section. **(A)** Periodic acid–Schiff–metanil yellow (PAS-MY), JB-4 medium; **(B)** PAS, paraffin medium; **(C)** toluidine blue, semithin section; **(D–G)** transmission electron microscopy (TEM). m, mucocyte; z, zooxanthella.

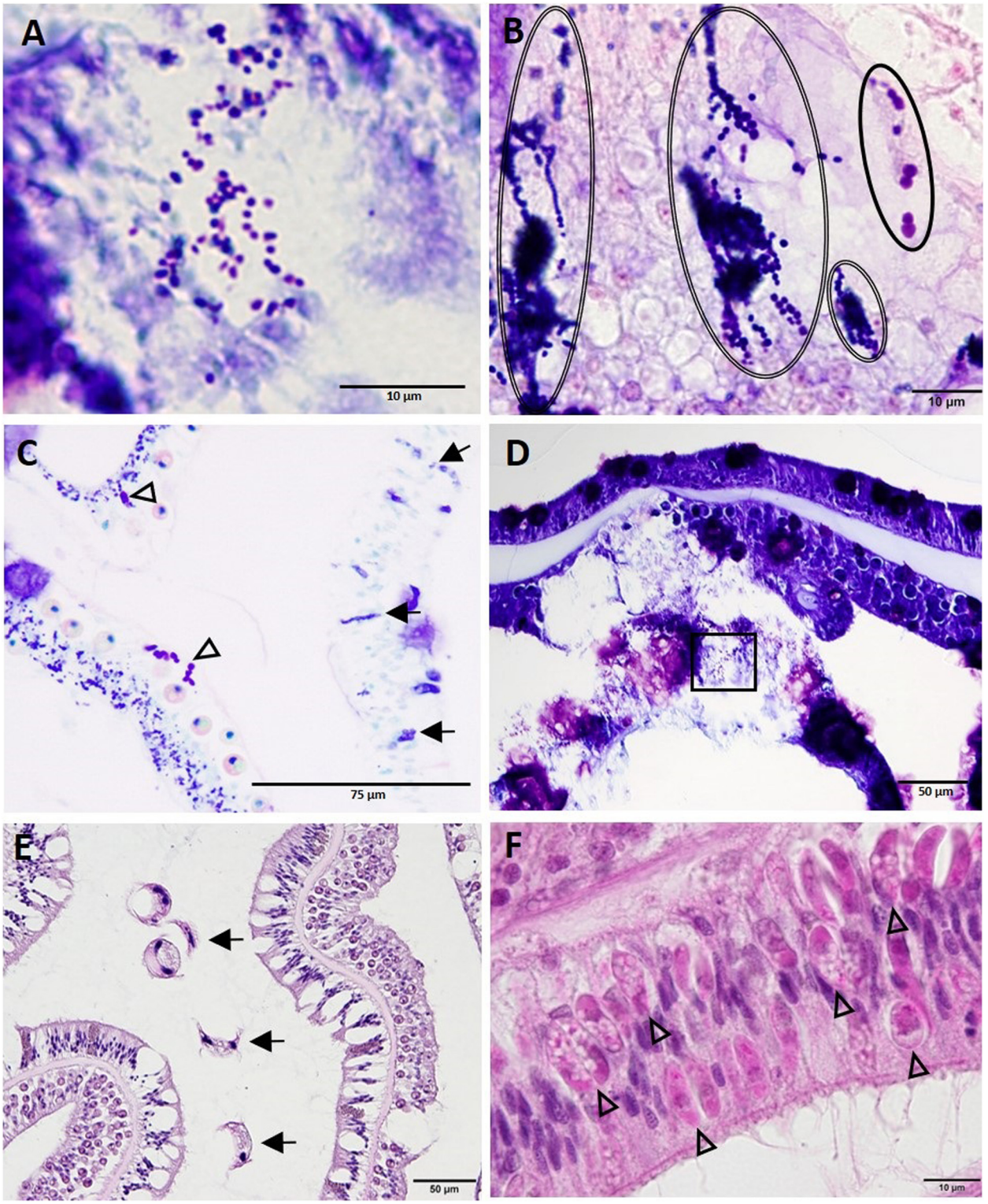

FIGURE 13 | Diverse coccoidlike structures and parasites. **(A)** High magnification of inset area marked in **(D)** shows coccoidlike structures in necrotic basal body wall (BBW) gastrodermis associated with lytic necrosis (LN) lesion in *Montastraea cavernosa*. **(B)** Coccoidlike structures (double-line ovals) and coccobacilloidlike structures (solid oval) in mesentery of apparently healthy tissue of *Diploria labyrinthiformis*. **(C)** Coccoidlike structures (arrows) in the epidermis and coccobacilloidlike structures (arrowheads) in the SBW gastrodermis of an apparently healthy area in *M. cavernosa*. **(D)** LN in BBW and SBW gastrodermis in *M. cavernosa* showing location of coccoidlike structures [inset shown in **(A)**]. **(E)** Surface of *Pseudodiploria strigosa* showing trichodinid ciliates (arrows). **(F)** Apicomplexan sporozoites (arrowheads) in the actinopharynx epidermis of *M. cavernosa*. **(A,D)** thionin; **(B,C)** Giemsa; **(E,F)** hematoxylin and eosin (H and E).

species. Endolithic organisms were occasionally observed penetrating or in close contact with the BBW of the coral tissue with advancing LN.

Prevalence of LN Lesions Across Species

Hallmark LN lesions were observed in samples collected from diseased (HD) and, to a lesser extent, unaffected areas on diseased colonies (HU), as well as in samples taken from apparently healthy colonies (HH) in disease-affected sites (**Table 1**). Of the samples showing diverse gross signs of acute, subacute, or chronic tissue loss (HD) evaluated across species (n = 82), a prevalence of 87% was confirmed histologically to have LN lesions. Of the samples (n = 79) collected in parallel from apparently unaffected (HU) areas on the same diseased colonies showing gross signs of SCTLD across species, a prevalence of 11% were confirmed histologically with LN lesions (**Table 1**). Of the apparently healthy (HH, n = 41) colonies evaluated from SCTLD sites, a prevalence of 15% had LN lesions. Samples collected from healthy (reference) sites (HH, n = 51) did not show LN lesions, except one *M. cavernosa* from Dustan Rocks (April 2017), in which early-stage LN was observed (**Table 1**; **Figures 6A,B,D**).

Lytic necrosis was seen in grossly lesioned and apparently normal tissues for most coral species in SCTLD sites regardless of health status. LN was observed histologically in all eight SCTLD-affected coral species, with high but varying prevalence levels in lesioned (HD) samples from *M. cavernosa* (n = 23, or 100%), *Meandrina meandrites* (n = 5, or 100%), *Diploria labyrinthiformis* (n = 2 or 100%), *P. strigosa* (n = 7/8, or 88%), *S. siderea* (n = 12/15, or 80%), *O. faveolata* (n = 10/13, or 77%), *C. natans* (n = 9/12, or 75%), and *Dendrogyra cylindrus* (n = 3/4, or 75%). For apparently normal samples from diseased colonies (HU) comprising seven species, prevalence was lower and LN seen only in *Diploria labyrinthiformis* (n = 1/2, or 50%), *S. siderea* (n = 4/16, or 25%), *Montastraea cavernosa* (n = 2/23, or 9%), *C. natans* (n = 1/11, or 9%), and *O. faveolata* (n = 1/12, or 8%). Of seven species of apparently healthy colonies from SCTLD sites with apparently normal tissues (HH), LN lesions were seen at low prevalence in *D. labyrinthiformis* (n = 1/1, or 100%), *O. faveolata* (n = 2/8, or 25%), and *S. siderea* (n = 2/9, or 22%) (**Table 1**).

DISCUSSION

The histopathology findings presented here indicate that SCTLD is a bottom-up process starting with pathological changes in BBW and SBW zooxanthellae with lesions first appearing in the gastrodermis of the BBW. In multiple coral species, lesions progress to loss of the BBW tissue followed by attendant tissue loss in adjacent SBW, leading to sloughing and a gross lesion of acute, subacute, or chronic tissue loss. Feasibly, the advancement of surface lesions and their progression at different rates of tissue loss in various coral species could be caused by secondary pathogens or opportunists that colonize following initiation of BBW LN lesions by still undetermined primary causal agents. Bacteria apparently play a role in SCTLD progression, as evidenced by the slowing of lesion progression after the application of antibiotics (Neely et al., 2020). While *Vibrio coralliilyticus* toxins have been detected in ∼20% of *M. cavernosa* with SCTLD[7], we saw no evidence that bacteria are the primary cause of SCTLD.

The consistency of the LN lesion across the scleractinian species examined here seems to be a unique phenomenon in coral TLDs, which, at least in the Pacific, present with myriad microscopic manifestations (Williams et al., 2011; Work and Aeby, 2011; Work et al., 2012; Rodríguez-Villalobos et al., 2015). The presence of lesions in the BBW of even apparently healthy corals also indicates that LN starts before the manifestation of gross lesions. This could have important ramifications for management protocols that assess the health of corals based on their gross visual appearance alone and may require additional action (e.g., quarantine) before corals can be approved for transplantation, rescue, or coral-restoration purposes (Hein et al., 2017). Specifically, even apparently normal-appearing corals may not be healthy, and additional tests including, at least, microscopic examinations of tissue might be necessary in evaluating whether corals are SCTLD-free prior to such management actions. The possible early LN lesion from an *M. cavernosa* sample collected in April 2017 from a reference site in Dustan Rocks could be a significant finding, as it would place SCTLD in the Middle Keys months earlier than has been documented. If this sample does indeed represent SCTLD (although further screening is required of "healthy" colonies in SCTLD-endemic zones), then the development of diagnostic tests for SCTLD in corals in which no surface lesions are evident is further merited.

Tissue loss diseases, including SCTLD, in the Caribbean are increasingly notorious for causing coral declines (Porter et al., 2001; Neely and Lewis, 2020). During the early appearance of SCTLD in the Florida Reef Tract (Precht et al., 2016; Gintert et al., 2019), researchers considered that this disease was the same as or similar to WP (or variants) reported in mostly the same coral species in Florida (Dustan, 1977; Richardson, 1998; Richardson et al., 1998a,b; Porter et al., 2001) and in the Caribbean, where ∼ 40 species have been affected (Green and Bruckner, 2000; Weil, 2004). Another grossly similar disease to SCTLD, reported in June 2008 from the Dry Tortugas (Tortugas multispecies rapid TLD [TMRTLD], Brandt et al., 2012), affected similar scleractinian species. However, absent systematic histopathology descriptions, it is difficult to compare SCTLD to these other TLDs, illustrating the confusion that can arise when coral diseases are described based only on gross lesions (Work and Aeby, 2006).

Based on TEM observations in more than 80% of the WP tissue grids examined, Borger (2003) described LN below the epidermis in *C. natans* and *S. siderea* and suggested that the lesions might be caused by toxicoses associated with bacterial or fungal infections, associated anoxia, or endo- or exotoxins. Additionally, in a brief report showing histologic lesions of presumed WP in *Dichocoenia stokesii* from Navassa Island, in the Caribbean, and *O. faveolata* from Puerto Rico, Galloway et al. (2007) revealed diffuse gastrodermal necrosis that appeared

[7]https://floridadep.gov/rcp/coral/documents/studies-ecology-and-microbiology-floridas-coral-tissue-loss-diseases

to be markedly similar to the LN lesions described here. In a historical context, and to assess whether SCTLD has been documented (as WP or TMRTLD) on a smaller scale since the late 1970s, unraveling the relationship between these diseases is relevant. Assuming that SCTLD somehow originated in 2014 may be misleading if the disease is instead the re-emergence of a previously documented TLD.

Although SCTLD can manifest with varying rates of tissue loss, colonies of most species show a noticeable area of recent necrosis (indicated by intact bare, white skeleton) following the tissue-loss margin before overgrowth by turf algae on the exposed skeleton. Grossly, *S. siderea* colonies displayed a characteristic pink discoloration that can be challenging to discern from dark spot syndrome (Santavy et al., 2001) or other undescribed lesions. In *Siderastrea* spp. showing marked variability in pink pigmentation associated with bleaching, Sassi et al. (2015) reported that pocilloporin fluorescent pigments became visible in the deeper tissue layers with reduced zooxanthellae densities (as described by Bongiorni and Rinkevich, 2005). Perhaps similar mechanisms exist for *S. siderea* with SCTLD.

Given that SCTLD is a breakdown of host–symbiont relationships, understanding whether the process starts with the symbiont or the coral host cells seems of paramount importance. Feasibly, different genera of Symbiodiniaceae may be more susceptible to SCTLD than others and if so, this may explain the apparent range of coral species affected, with some species unaffected to others being highly affected. Functional Symbiodiniaceae species differences across tissue compartments have not been assessed and perhaps zooxanthellae located deeper in tissue, with less access to light (or sensitive to other abiotic or biotic factors), are more susceptible to whatever etiology is causing SCTLD. In summary, the fact that zooxanthellae are initially affected provides an important clue.

Environmental stress can cause loss of zooxanthellae from the gastrodermis, via multiple modes of death including host-cell detachment, necrosis, apoptosis, symbiophagy, or exocytosis, resulting in coral bleaching (Gates et al., 1992; Dunn et al., 2007; Weis, 2008; Downs et al., 2009, 2013; Hanes and Kempf, 2013; Paxton et al., 2013; Camaya et al., 2016; Dani et al., 2016). For symbiont mortality during coral diseases, such mechanistic changes have been less well studied (Cervino et al., 2004; Hauff et al., 2014). Bacterial pathogens can initiate a non-specific xenophagic response in the coral that could also include zooxanthellae (symbiophagy) (Downs et al., 2009). Symbiophagy and associated necrosis were triggered by a bacterial infection in the hydrocoral *Millepora dichotoma* exhibiting multifocal lesions that grossly appeared to be bleached (Paramasivam et al., 2013).

A plausible cause of SCTLD, based on light microscopic findings, is toxicosis. Perhaps toxins selective to zooxanthellae or host cells are responsible for symbiont breakdown. For instance, free-living dinoflagellates produce diverse toxins and bioactive compounds with an array of effects on aquatic animals (Landsberg, 2002). Toxin production can be intermittent and driven by abiotic factors (e.g., temperature, nutrients) or biotic factors (e.g., allelopathy, predation) (Cembella and John, 2006). Symbiotic dinoflagellate zooxanthellae also produce secondary metabolites (e.g., zooxanthellatoxins) that have diverse bioactivities *in vitro* (Nakamura et al., 1993; Fukatsu et al., 2007; Beedessee et al., 2015, 2019), but little is known of the function of these natural compounds in their coral hosts (Gordon and Leggat, 2010) or of any negative effects they may have (McConnaughey, 2012). Plausibly, zooxanthellae could become toxic to the host, leading to the initiation of SCTLD. Lytic necrosis is reminiscent of lesions caused by bioactive lytic compounds, such as proteases, more typically associated with bacterial pathogens (Miyoshi and Shinoda, 2000; Newman and Clements, 2008). The possible role of biogenic toxins or allelochemicals from other coral-associated organisms warrants consideration.

Zooxanthellae also produce various metabolites that can disrupt symbiosis. In response to environmental stress or exposure to pathogens, increased production by zooxanthellae of, for example, reactive oxygen species (ROS), nitric oxide, antioxidants such as dimethyl-sulfoniopropionate, and volatile organic compounds could play a role in the death of zooxanthellae and host coral cells (Mydlarz and Jacobs, 2004; Bouchard and Yamasaki, 2008; Mydlarz et al., 2009; Hawkins and Davy, 2012; McGinty et al., 2012; McLenon and DiTullio, 2012; Caruana and Malin, 2014; Wietheger et al., 2018; Lawson et al., 2019; Zhou et al., 2019). As part of their innate immune response against pathogens, corals also produce antioxidants such as melanin, with synthesis activated by cleavage of prophenoloxidase to phenoloxidase (PO) (Palmer et al., 2008). ROS produced during this process can be cytotoxic to pathogens but can also cause self-harm unless countered by antioxidants (Wright et al., 2017). In diseased and healthy colonies of *Acropora millepora* with the TLD white syndrome, increased PO activity was detected at the lesion border (Palmer et al., 2011). The putative detection of melanin by FM stain, shown here (**Figures 7E,F**) in degrading zooxanthellae closely associated with LN lesions, might indicate a pathological response to excess ROS, but more research would be beneficial.

Potential pathogens of zooxanthellae may also be causal factors. Bacteria (Ritchie, 2011; Bernasconi et al., 2019) and viruses in zooxanthellae have been documented (Wilson et al., 2005; Lohr et al., 2007) and associated with bleaching (Correa et al., 2016) and TLDs (Lawrence et al., 2014, 2015; Soffer et al., 2014), but Koch's postulates have yet to be met (Thrusfield, 2016). Initial evaluation by TEM of zooxanthellae from *Montastraea cavernosa* in this study revealed no discernible viral particles. But further ultrastructural examination of corals is clearly needed if viruses are to be ruled out as a cause of SCTLD.

Zooxanthella immune dysfunction may also be a significant contributory factor to SCTLD. For example, plants have a well-characterized immune response, but upon exposure to certain insults their hypersensitivity response leads to cell death (Jones and Dangl, 2006; Coll et al., 2011; Leary et al., 2018). Another mechanism, one whereby the host–symbiont relationship is disrupted, could be operating if zooxanthellae can suppress host immunity (Merselis et al., 2018) or if the host cell no longer recognizes the endosymbiont as self, leading to degradation and death of zooxanthellae. Sorting these processes out, however, would require much deeper understanding of coral host-cell

immunity, a field still in its infancy (Mydlarz et al., 2006, 2016; Palmer and Traylor-Knowles, 2012).

Finally, the Florida coast has had a long history of watershed alteration and pollution, with significant effects on corals (Rogers, 1990; Marubini and Davies, 1996; Lipp et al., 2002; Downs et al., 2005; Wagner et al., 2010). Associated factors, such as contaminants, pesticides, toxicants, nutrients, and sedimentation, may selectively kill or stress zooxanthellae (Owen et al., 2003; Reichelt-Brushett and McOrist, 2003; Brodie et al., 2012), but their role, if any, in coral disease has been less well studied. All these factors would be fruitful avenues of investigation.

Although the spatial epidemiology patterns (Muller et al., 2020) and the apparent efficacy of antimicrobial treatments on lesions (Aeby et al., 2019; Neely et al., 2020) indicate that SCTLD is infectious, no evidence was visible at the light microscopic or ultrastructural level of infectious agents consistently associated with symbiont–host disruption. Although pathogenic microorganisms may not necessarily be observed histologically, the assumptions based on previous studies that Koch's postulates have been fulfilled by repeatedly isolating and culturing the same candidate microorganism from a lesion, recreating the lesion experimentally with that organism, and then re-isolating the microorganism (Rosenberg, 2004), are often done in the absence of histopathological confirmation of the primary pathogen in co-associated early lesions (Arboleda and Reichardt, 2010). Lesions can be recreated with pathogenic bacteria, but they do not necessarily prove they cause the same disease, especially if as in corals, many TLDs grossly appear the same (Work and Aeby, 2006). That some diseases have not subsequently been recreated, nor the purported primary pathogen again detected, has also led to confusion as to the correct etiology of some coral diseases (Sunagawa et al., 2009a; Sutherland et al., 2016).

Additionally, an obvious host-cell inflammatory response (e.g., amebocytes) was not seen in histopathology of SCTLD, as might have been expected if corals were targeting pathogens (Mydlarz et al., 2008). Thus, while the identities of the coccoidlike and coccobacilloidlike structures need to be confirmed, bacteria, fungi, and parasites can initially be ruled out as proximate causes of SCTLD. But not all virus-induced lesions at the microscopic level will show viral particles (Russell et al., 2008), and a role for viruses in affecting either the corals or their zooxanthellae remains a possibility. Indeed, the commonality among the multiple coral species susceptible to SCTLD may lie not with the corals themselves but with their associated zooxanthellae, which are less diverse than affected corals at the genus level.

Although SCTLD can be recreated experimentally (Aeby et al., 2019) this does not necessarily lead to the conclusion that the disease is caused by an infectious microorganism, although exposure of healthy coral fragments to an SCTLD-affected fragment elicits tissue loss, indicating that a transmissible pathogen is involved. Perhaps corals with SCTLD experimentally transmit "non-self" organisms or allelochemicals that induce a host response that initiates lesion formation. Secondary opportunistic bacteria can still play a role in lesion advancement. Finally, although this seems less likely because of documented experimental transmission, SCTLD may result from an environmental co-factor or cause, as postulated with sea star wasting disease (SSWD). Originally thought to be transmissible and infectious based on field and molecular data, no compelling link between viruses and cell death has been made at the cellular level, except possibly in one sea star species (Hewson et al., 2014, 2018), and at least 10 different densoviruses (primary suspect pathogen) have been found to be equally represented in symptomatic and asymptomatic sea stars (Jackson et al., 2020). Although the etiology is still unknown, one possibility is that SSWD is caused by temperature anomalies or other environmental factors (Hewson et al., 2018).

If the BBW gastrodermis is the first compartment to be affected in SCTLD, understanding how this process is initiated may be difficult to discern. In contrast to zooxanthellae, much less is known about the cell types that make up tissue compartments in corals. Although the basic layers (calicodermis, gastrodermis, mesoglea, epidermis) have been well documented, as are certain cell types such as cnidae (Peters, 2016), little is known about the complex physiological interactions between zooxanthellae and their host cells that would result in the pathology changes seen here. Nor is it clear whether initiation of LN in the BBW might be driven by influences from the calicodermis–skeleton interface or the GVC. For example, various macromolecules involved in skeletal calcification or digestion are enzymatic, lytic, or possibly toxic (Ramos-Silva et al., 2013; Deutekom et al., 2016; Raz-Bahat et al., 2017). Development of animal models for diseases of cnidarians might help in understanding fundamental cellular processes, for example, models utilizing *Exaiptasia pallida* (Weis et al., 2008; Sunagawa et al., 2009b) or *Hydra viridissima* (Kovacevic, 2012).

Other changes in corals in the present study were considered secondary. The CIBs found only in *M. cavernosa* and *P. strigosa* were inconsistently associated with LN lesions in the BBW, and their function is unknown. Diverse CIBs (e.g., organic crystalline metabolites) are often found in normal organisms (Edwardson and Christie, 1978; Nürnberger et al., 2017) and while the CIBs reported here are similar in ultrastructural appearance to the kalisomes in the gastrodermis of coral larvae (e.g., *Pocillopora damicornis*) (Clode and Marshall, 2002), they could be crystalline inclusions resembling aragonite calcium carbonate (Hayes and Goreau, 1977), and still have to be analyzed chemically. When crystallized in the laboratory at pH 8.0, the coral chromoprotein pocilloporin forms a mauve tetrahedron (Beddoe et al., 2003) reminiscent of the CIBs noted here, but it is not known whether this process would occur in corals *in situ*. Among other biological roles, pocilloporins are thought to be ROS scavengers (Bou-Abdallah et al., 2006; Furla et al., 2011), which could relate to the symbiont–host physiological dysfunctions mentioned previously. Finally, some of the parasites (e.g., *Halofolliculina* sp. ciliates) noted here in corals with SCTLD are likely incidental following skeletal exposure. Ciliates have been associated with TLD lesions in the Pacific (Work et al., 2012) and in the Caribbean (Verde et al., 2016). Of particular interest are the trichodinid ciliates not reported previously in corals and the epidermal apicomplexans. An apicomplexan coccidian in corals has been described (Upton and Peters, 1986), and,

while other apicomplexans have been reported (Kirk et al., 2013; Kwong et al., 2019), whether they are pathogenic is unknown.

In summary, SCTLD may have a non-infectious primary etiology (with a likely role for secondary opportunists or pathogens), but much remains to be done to unravel the actual cause. Improving understanding of how the disease progresses among species by using histology to monitor changes over time might refine the case response for individual species, some of which appear more susceptible than others. Developing an animal model for coral diseases and immune function would also elucidate mechanisms of disease and responses to insults by both coral and symbiont. Additional ultrastructural and molecular studies might allow for the detection of viruses and better understanding of interactions between hosts and symbionts at different stages of disease. While scientists continue to understand the causes of SCTLD, broader management activities to reduce stresses to coral reefs such as reductions in land based pollution (Fabricius, 2005) could benefit coral reefs in Florida.

DATA AVAILABILITY STATEMENT

The raw data supporting the conclusions of this article will be made available by the authors, without undue reservation.

AUTHOR CONTRIBUTIONS

JL secured funding. JL, YK, and EP designed the research. YK prepared samples for histology. PW, NP, and YW conducted histology and special staining. JL and YK performed TEM. KM and LH managed collections and field data. JL, YK, EP, and TW evaluated histological slides and interpreted histopathology. JL and TW drafted the manuscript. All authors contributed to writing the manuscript.

FUNDING

This research was supported by U.S. Fish and Wildlife Service Funds for State Wildlife Grant Award FL-T-F18AF00492 awarded to FWC and supplemented by funding to FWC for field collections from the Florida Coastal Office, Florida Department of Environmental Protection Coral Reef Conservation Program (order numbers BOA35A and B25636).

ACKNOWLEDGMENTS

Many thanks to the FWC-FWRI core field sample collections staff: Nathan Berkebile, Michael Bollinger, Vanessa Brinkhuis, Katy Cummings, Ananda Ellis, Kristine Fisher, John Hart, Brian Reckenbeil, and Jennifer Stein. Paul Barbera, Tiffany Boisvert, Stephanie Schopmeyer, and William Sharp (FWC-FWRI), Sierra Hobbs (University of West Florida), Elizabeth McDonald and Karen Neely (Nova Southeastern University), Kristi Kerrigan (Florida Department of Environmental Protection), and Jason Spadaro (College of the Florida Keys) also provided assistance or operational support for the collection of coral samples. We also thank FWC-FWRI staff Michelle Franco for histological support, Clark Gray for TEM assistance, and Lauren Gentry for designing **Figure 1**. Collections were authorized under FWC special activity license SAL-17-1702-SRP, and Florida Keys National Marine Sanctuary permits: FKNMS-2016-078, FKNMS-2017-100, FKNMS-2018-006, and FKNMS-2015-156. Mention of products and trade names does not imply endorsement by the United States Government.

REFERENCES

Aeby, G. S., Ushijima, B., Campbell, J. E., Jones, S., Williams, G., Meyer, J. L., et al. (2019). Pathogenesis of a tissue loss disease affecting multiple species of corals along the Florida reef tract. *Front. Mar. Sci.* 6:00678. doi: 10.3389/fmars.2019.00678

Alvarez-Filip, L., Estrada-Saldívar, N., Pérez-Cervantes, E., Molina-Hernández, A., and Gonzalez-Barrios, F. J. (2019). A rapid spread of the stony coral tissue loss disease outbreak in the Mexican Caribbean. *PeerJ* 7:e8069. doi: 10.7717/peerj.8069

Arboleda, M. D., and Reichardt, W. T. (2010). Vibrio sp. *causing Porites ulcerative white spot disease*. *Dis. Aquat. Org.* 90, 93–104. doi: 10.3354/dao02222

Aronson, R. B., and Precht, W. F. (2001). White-band disease and the changing face of Caribbean coral reefs. *Hydrobiology* 460, 25–38. doi: 10.1007/978-94-017-3284-0_2

Beddoe, T., Ling, M., Dove, S., Hoegh-Guldberg, O., Devenish, R. J., Prescott, M., et al. (2003). The production, purification and crystallization of a pocilloporin pigment from a reef-forming coral. *Acta Crystallogr. D* 59, 597–599. doi: 10.1107/s0907444902023466

Beedessee, G., Hisata, K., Roy, M. C., Satoh, N., and Shoguchi, E. (2015). Multifunctional polyketide synthase genes identified by genomic survey of the symbiotic dinoflagellate. *Symbiodinium minutum*. *BMC Genomics* 16:941. doi: 10.1186/s12864-015-2195-8

Beedessee, G., Hisata, K., Roy, M. C., Van Dolah, F. M., Satoh, N., and Shoguchi, E. (2019). Diversified secondary metabolite biosynthesis gene repertoire revealed in symbiotic dinoflagellates. *Sci. Rep.* 9, 1–12. doi: 10.1038/s41598-018-37792-0

Bernasconi, R., Stat, M., Koenders, A., and Huggett, M. J. (2019). Global networks of *Symbiodinium*-bacteria within the coral holobiont. *Microb. Ecol.* 77, 794–807. doi: 10.1007/s00248-018-1255-4

Bongiorni, L., and Rinkevich, B. (2005). The pink-blue spot syndrome in *Acropora eurystoma* (Eilat, Red Sea): a possible marker of stress? *Zoology* 108, 247–256. doi: 10.1016/j.zool.2005.05.002

Borger, J. L. (2003). *Scleractinian Coral Diseases in South Florida and Dominica (West Indies): Epizootiology and Effects on Host Tissue Structure and Reproduction*. Ph.D. Dissertation, University of Miami, Miami, FL.

Bou-Abdallah, F., Chasteen, N. D., and Lesser, M. P. (2006). Quenching of superoxide radicals by green fluorescent protein. *Biochim. Biophys. Acta* 1760, 1690–1695. doi: 10.1016/j.bbagen.2006.08.014

Bouchard, J. N., and Yamasaki, H. (2008). Heat stress stimulates nitric oxide production in *Symbiodinium microadriaticum*: a possible linkage between nitric oxide and the coral bleaching phenomenon. *Plant Cell. Physiol.* 49, 641–652. doi: 10.1093/pcp/pcn037

Brandt, M. E., Ruttenberg, B. I., Waara, R., Miller, J., Witcher, B., Estep, A. J., et al. (2012). Dynamics of an acute coral disease outbreak associated with the macroalgae *Dictyota* spp. in dry tortugas national park. Florida, USA. *Bull. Mar. Sci.* 88, 1035–1050. doi: 10.5343/bms.2011.1104

Brodie, J. E., Kroon, F. J., Schaffelke, B., Wolanski, E. C., Lewis, S. E., Devlin, M. J., et al. (2012). Terrestrial pollutant runoff to the Great Barrier Reef: an update

of issues, priorities and management responses. *Mar. Pollut. Bull.* 65, 81–100. doi: 10.1016/j.marpolbul.2011.12.012

Bruckner, A. W. (2016). "White syndromes of western Atlantic reef-building corals," in *Diseases of Coral*, eds C. M. Woodley, C. A. Downs, A. W. Bruckner, J. W. Porter, and S. B. Galloway (Hoboken, NJ: John Wiley & Sons Inc), 316–332. doi: 10.1002/9781118828502.ch22

Camaya, A. P., Sekida, S., and Okuda, K. (2016). Changes in the ultrastructures of the coral *Pocillopora damicornis* after exposure to high temperature, ultraviolet and far-red radiation. *Cytology* 81, 465–470. doi: 10.1508/cytologia.81.465

Caruana, A. M. N., and Malin, G. (2014). The variability in DMSP content and DMSP lyase activity in marine dinoflagellates. *Progr. Oceanogr.* 120, 410–424. doi: 10.1016/j.pocean.2013.10.014

Cembella, A., and John, U. (2006). "Molecular physiology of toxin production and growth regulation in harmful algae," in *Ecology of Harmful Algae*, eds E. Granéli and J. T. Turner (Berlin: Springer Verlag), 215–227. doi: 10.1007/978-3-540-32210-8_17

Cervino, J. M., Hayes, R., Goreau, T. J., and Smith, G. W. (2004). Zooxanthellae regulation in yellow blotch/band and other coral diseases contrasted with temperature related bleaching: in situ destruction vs expulsion. *Symbiosis* 37, 63–85.

Clode, P. L., and Marshall, A. T. (2002). Kalisomes in corals: a novel KCl concentrating organelle? *Tissue Cell* 34, 199–209. doi: 10.1016/s0040-8166(02)00033-2

Coles, S. L., and Jokiel, P. L. (1977). Effects of temperature on photosynthesis and respiration in hermatypic corals. *Mar. Biol.* 4, 209–216. doi: 10.1007/BF00402313

Coll, N. S., Epple, P., and Dangl, J. L. (2011). Programmed cell death in the plant immune system. *Cell Death Differ.* 18, 1247–1256. doi: 10.1038/cdd.2011.37

Correa, A. M., Ainsworth, T. D., Rosales, S. M., Thurber, A. R., Butler, C. R., and Vega Thurber, R. L. (2016). Viral outbreak in corals associated with an in situ bleaching event: atypical herpes-like viruses and a new megavirus infecting *Symbiodinium*. *Front. Microbiol.* 7:127. doi: 10.3389/fmicb.2016.00127

Dani, V., Priouzeau, F., Pagnotta, S., Carette, D., Laugier, J.-P., and Sabourault, C. (2016). Thermal and menthol stress induce different cellular events during sea anemone bleaching. *Symbiosis* 69, 175–192. doi: 10.1007/s13199-016-0406-y

Deutekom, E. S., Konglerd, P., Ramos-Silva, P., and Kaandorp, J. A. (2016). "From molecules to morphologies, a multiscale modeling approach to unravel the complex system of coral calcification," in *The Cnidaria, Past, Present and Future: The World of Medusa and Her Sisters*, eds S. Goffredo and Z. Dubinsky (Cham: Springer International Publishing), 223–236. doi: 10.1007/978-3-319-31305-4_14

Downs, C. A., Fauth, J. E., Robinson, C. E., Curry, R., Lanzendorf, B., Halas, J. C., et al. (2005). Cellular diagnostics and coral health: declining coral health in the Florida Keys. *Mar. Pollut. Bull.* 51, 558–569. doi: 10.1016/j.marpolbul.2005.04.017

Downs, C. A., Kramarsky-Winter, E., Martinez, J., Kushmaro, A., Woodley, C. M., Loya, Y., et al. (2009). Symbiophagy as a cellular mechanism for coral bleaching. *Autophagy* 5, 211–216. doi: 10.4161/auto.5.2.7405

Downs, C. A., McDougall, K. E., Woodley, C. M., Fauth, J. E., Richmond, R. H., Kushmaro, A., et al. (2013). Heat-stress and light-stress induce different cellular pathologies in the symbiotic dinoflagellate during coral bleaching. *PLoS One* 8:e77173. doi: 10.1371/journal.pone.0077173

Dunn, S. R., Schnitzler, C. E., and Weis, V. M. (2007). Apoptosis and autophagy as mechanisms of dinoflagellate symbiont release during cnidarian bleaching: every which way you lose. *Proc. Roy. Soc. B Biol. Sci.* 274, 3079–3085. doi: 10.1098/rspb.2007.0711

Dustan, P. (1977). Vitality of reef coral populations off Key Largo, Florida: recruitment and mortality. *Environ. Geol.* 2, 51–58. doi: 10.1007/BF02430665

Edwardson, J. R., and Christie, R. G. (1978). Use of virus-induced inclusions in classification and diagnosis. *Ann. Rev. Phytopathol.* 16, 31–55. doi: 10.1146/annurev.py.16.090178.000335

Fabricius, K. E. (2005). Effects of terrestrial runoff on the ecology of corals and coral reefs: review and synthesis. *Mar. Pollut. Bull.* 50, 125–146. doi: 10.1016/j.marpolbul.2004.11.028

Fukatsu, T., Onodera, K., Ohta, Y., Oba, Y., Nakamura, H., Shintani, T., et al. (2007). Zooxanthellamide D, a polyhydroxy polyene amide from a marine dinoflagellate, and chemotaxonomic perspective of the *Symbiodinium* polyols. *J. Nat. Prod.* 70, 407–411. doi: 10.1021/np060596p

Furla, P., Richier, S., and Allemand, D. (2011). "Physiological adaptation to symbiosis in cnidarians," in *Coral Reefs: An Ecosystem in Transition*, eds Z. Dubinsky and N. Stambler (Dordrecht: Springer), 187–195. doi: 10.1007/978-94-007-0114-4_12

Galloway, S. B., Work, T. M., Bochsler, V. S., Harley, R. A., Kramarsky-Winters, E., McLaughlin, S. M., et al. (2007). *Coral Disease and Health Workshop: Coral Histopathology II*. NOAA Technical Memorandum NOS NCCOS 56 and CRCP 4. Silver Spring, MD: NOAA.

Gates, R. D., Baghdasarian, G., and Muscatine, L. (1992). Temperature stress causes host cell detachment in symbiotic cnidarians: implications for coral bleaching. *Biol. Bull.* 182, 324–332. doi: 10.2307/1542252

Gignoux-Wolfsohn, S. A., Precht, W. F., Peters, E. C., Gintert, B. E., and Kaufman, L. S. (2020). Ecology, histopathology, and microbial ecology of a white-band disease outbreak in the threatened staghorn coral *Acropora cervicornis*. *Dis. Aquat. Org.* 137, 217–237. doi: 10.3354/dao03441

Gintert, B. E., Manzello, D. P., Enochs, I. C., Kolodziej, G., Carlton, R., Gleason, A. C., et al. (2018). Marked annual coral bleaching resilience of an inshore patch reef in the Florida Keys: a nugget of hope, aberrance, or last man standing? *Coral Reefs* 37, 533–547. doi: 10.1007/s00338-018-1678-x

Gintert, B. E., Precht, W. F., Fura, R., Rogers, K., Rice, M., Precht, L. L., et al. (2019). Regional coral disease outbreak overwhelms impacts from a local dredge project. *Environ. Monitor. Assess.* 191:630. doi: 10.1007/s10661-019-7767-7

Gordon, B. R., and Leggat, W. (2010). *Symbiodinium*–invertebrate symbioses and the role of metabolomics. *Mar. Drugs* 8, 2546–2568. doi: 10.3390/md8102546

Green, E. P., and Bruckner, A. W. (2000). The significance of coral disease epizootiology for coral reef conservation. *Biol. Conserv.* 96, 347–361. doi: 10.1016/S0006-3207(00)00073-2

Hanes, S. D., and Kempf, S. C. (2013). Host autophagic degradation and associated symbiont loss in response to heat stress in the symbiotic anemone. *Aiptasia pallida*. *Invert. Biol.* 132, 95–107. doi: 10.1111/ivb.12018

Hauff, B., Cervino, J. M., Haslun, J. A., Krucher, N., Wier, A. M., Mannix, A. L., et al. (2014). Genetically divergent *Symbiodinium* sp. display distinct molecular responses to pathogenic Vibrio and thermal stress. *Dis. Aquat. Org.* 112, 149–159. doi: 10.3354/dao02802

Hawkins, T. D., and Davy, S. K. (2012). Nitric oxide production and tolerance differ among *Symbiodinium* types exposed to heat stress. *Plant Cell Physiol.* 53, 1889–1898. doi: 10.1093/pcp/pcs127

Hayes, R. L., and Goreau, N. I. (1977). Intracellular crystal-bearing vesicles in the epidermis of scleractinian corals, *Astrangia danae* (Agassiz) and *Porites porites* (Pallas). *Biol. Bull.* 152, 26–40. doi: 10.2307/1540724

Hein, M. Y., Willis, B. L., Beeden, R., and Birtles, A. (2017). The need for broader ecological and socioeconomic tools to evaluate the effectiveness of coral restoration programs. *Restor. Ecol.* 25, 873–883. doi: 10.1111/rec.12580

Hewson, I., Bistolas, K. S., Quijano Cardé, E. M., Button, J. B., Foster, P. J., Flanzenbaum, J. M., et al. (2018). Investigating the complex association between viral ecology, environment, and northeast Pacific sea star wasting. *Front. Mar. Sci.* 5:77. doi: 10.3389/fmars.2018.00077

Hewson, I., Button, J. B., Gudenkauf, B. M., Miner, B. G., Newton, A. L., Gaydos, J. K., et al. (2014). Densovirus associated with sea-star wasting disease and mass mortality. *Proc. Natl. Acad. Sci. U.S.A.* 111, 17278–17283. doi: 10.1073/pnas.1416625111

Jackson, E. W., Wilhelm, R. C., Johnson, M. R., Lutz, H. L., Danforth, I., Gaydos, J. K., et al. (2020). Diversity of sea star-associated densoviruses and transcribed endogenized viral elements of densovirus origin. *bioRxiv[Preprint]*. doi: 10.1101/2020.08.05.239004

Jones, J. D. G., and Dangl, J. L. (2006). The plant immune system. *Nature* 444, 323–329. doi: 10.1038/nature05286

Jones, M. V., and Calabresi, P. A. (2007). Agar-gelatin for embedding tissues prior to paraffin processing. *Biotechnology* 42, 569–570. doi: 10.2144/000112456

Kirk, N. L., Thornhill, D. J., Kemp, D. W., Fitt, W. K., and Santos, S. R. (2013). Ubiquitous associations and a peak fall prevalence between apicomplexan symbionts and reef corals in Florida and the Bahamas. *Coral Reefs* 32, 847–858. doi: 10.1007/s00338-013-1038-9

Kovacevic, G. (2012). Value of the *Hydra* model system for studying symbiosis. *Int. J. Dev. Biol.* 56, 627–635. doi: 10.1387/ijdb.123510gk

Kuta, K. G., and Richardson, L. L. (1996). Abundance and distribution of black band disease on coral reefs in the northern Florida Keys. *Coral Reefs* 15, 219–223. doi: 10.1007/bf01787455

Kwong, W. K., del Campo, J., Mathur, V., Vermeij, M. J., and Keeling, P. J. (2019). A widespread coral-infecting apicomplexan with chlorophyll biosynthesis genes. *Nature* 568, 103–107. doi: 10.1038/s41586-019-1072-z

Landsberg, J. H. (2002). The effects of harmful algal blooms on aquatic organisms. *Rev. Fish. Sci.* 10, 113–390. doi: 10.1080/20026491051695

Lawrence, S. A., Davy, J. E., Wilson, W. H., Hoegh-Guldberg, O., and Davy, S. K. (2015). *Porites* white patch syndrome: associated viruses and disease physiology. *Coral Reefs* 34, 249–257. doi: 10.1007/s00338-014-1218-2

Lawrence, S. A., Wilson, W. H., Davy, J. E., and Davy, S. K. (2014). Latent virus-like infections are present in a diverse range of *Symbiodinium* spp. *(Dinophyta). J. Phycol.* 50, 984–997. doi: 10.1111/jpy.12242

Lawson, C. A., Possell, M., Seymour, J. R., Raina, J.-B., and Suggett, D. J. (2019). Coral endosymbionts (Symbiodiniaceae) emit species-specific volatilomes that shift when exposed to thermal stress. *Sci. Rep.* 9:17395. doi: 10.1038/s41598-019-53552-0

Leary, A. Y., Sanguankiattichai, N., Duggan, C., Tumtas, Y., Pandey, P., Segretin, M. E., et al. (2018). Modulation of plant autophagy during pathogen attack. *J. Exp. Bot.* 69, 1325–1333. doi: 10.1093/jxb/erx425

Lessios, H. A. (1988). Mass mortality of *Diadema antillarum* in the Caribbean: what have we learned? *Annu. Rev. Ecol. Syst.* 19, 371–393. doi: 10.1146/annurev.es.19.110188.002103

Lessios, H. A. (2016). The great *Diadema antillarum* die-off: 30 years later. *Annu. Rev. Mar. Sci.* 8, 267–283. doi: 10.1146/annurev-marine-122414-033857

Lipp, E. K., Jarrell, J. L., Griffin, D. W., Lukasik, J., Jacukiewicz, J., and Rose, J. B. (2002). Preliminary evidence for human fecal contamination in corals of the Florida Keys, USA. *Mar. Pollut. Bull.* 44, 666–670. doi: 10.1016/S0025-326X(01)00332-0

Lohr, J., Munn, C. B., and Wilson, W. H. (2007). Characterization of a latent virus-like infection of symbiotic zooxanthellae. *Appl. Environ. Microbiol.* 73, 2976–2981. doi: 10.1128/AEM.02449-06

Luna, L. G. (1968). *Manual of Histologic Staining Methods of the Armed Forces Institutes of Pathology*, third edition. New York, NY: McGraw-Hill.

Manzello, D. P. (2015). Rapid recent warming of coral reefs in the Florida Keys. *Sci. Rep.* 5:16762. doi: 10.1038/srep16762

Marubini, F., and Davies, P. S. (1996). Nitrate increases zooxanthellae population density and reduces skeletogenesis in corals. *Mar. Biol.* 127, 319–328. doi: 10.1007/BF00942117

McConnaughey, T. A. (2012). Zooxanthellae that open calcium channels: implications for reef corals. *Mar. Ecol. Prog. Ser.* 460, 277–287. doi: 10.3354/meps09776

McDowell, E. M., and Trump, B. F. (1976). Histologic fixative suitable for diagnostic light and electron microscopy. *Arch. Pathol. Lab. Med.* 100, 405–414.

McGinty, E. S., Pieczonka, J., and Mydlarz, L. D. (2012). Variations in reactive oxygen release and antioxidant activity in multiple *Symbiodinium* types in response to elevated temperature. *Microb. Ecol.* 64, 1000–1007. doi: 10.1007/s00248-012-0085-z

McLenon, A., and DiTullio, G. (2012). Effects of increased temperature on dimethyl-sulfoniopropionate (DMSP) concentration and methionine synthase activity in *Symbiodinium microadriaticum*. *Biogeochemistry* 110, 17–29. doi: 10.1007/s10533-012-9733-0

Merselis, D. G., Lirman, D., and Rodriguez-Lanetty, M. (2018). Symbiotic immuno-suppression: is disease susceptibility the price of bleaching resistance? *PeerJ* 6:e4494. doi: 10.7717/peerj.4494

Meyer, J. L., Castellanos-Gell, J., Aeby, G. S., Häse, C. C., Ushijima, B., and Paul, V. J. (2019). Microbial community shifts associated with the ongoing stony coral tissue loss disease outbreak on the Florida reef tract. *Front. Microbiol.* 10:2244. doi: 10.3389/fmicb.2019.02244

Miller, M. W., Karazsia, J., Groves, C. E., Griffin, S., Moore, T., Wilber, P., et al. (2016). Detecting sedimentation impacts to coral reefs resulting from dredging the Port of Miami. *Florida USA*. *PeerJ* 4:e2711. doi: 10.7717/peerj.2711

Miller, M. W., Lohr, K. E., Cameron, C. M., Williams, D. E., and Peters, E. C. (2014). Disease dynamics and potential mitigation among restored and wild staghorn coral. *Acropora cervicornis*. *PeerJ* 2:e541. doi: 10.7717/peerj.541

Miyoshi, S., and Shinoda, S. (2000). Microbial metalloproteases and pathogenesis. *Microb. Infect.* 2, 91–98. doi: 10.1016/s1286-4579(00)00280-x

Mueller, E., Peters, E. C., Porter, J. W., and Porter, K. G. (2001). *Etiology and Distribution of Coral Diseases in the Florida Keys National Marine Sanctuary*. Available online at: http://ocean.floridamarine.org/FKNMS_WQPP/docs/cremp/reports/2001_Mueller_E_EtAl_Etiology_and_Distribution_Coral_Diseases_FKNMS.pdf (accessed May 4, 2020).

Muller, E. M., Sartor, C., Alcaraz, N. I., and van Woesik, R. (2020). Spatial epidemiology of the stony-coral-tissue loss disease in Florida. *Front. Mar. Sci.* 7:163. doi: 10.3389/fmars.2020.00163

Mydlarz, L. D., Couch, C. S., Weil, E., Smith, G., and Harvell, C. D. (2009). Immune defenses of healthy, bleached and diseased *Montastraea faveolata* during a natural bleaching event. *Dis. Aquat. Org.* 87, 67–78. doi: 10.3354/dao02088

Mydlarz, L. D., Fuess, L., Mann, W., Pinzón, J. H., and Gochfeld, D. J. (2016). "Cnidarian immunity: from genomes to phenomes," in *The Cnidaria, Past, Present and Future: The World of Medusa and Her Sisters*, eds S. Goffredo and Z. Dubinsky (Cham: Springer), 441–466. doi: 10.1007/978-3-319-31305-4_28

Mydlarz, L. D., Holthouse, S. F., Peters, E. C., and Harvell, C. D. (2008). Cellular responses in sea fan corals: granular amoebocytes react to pathogen and climate stressors. *PLoS One* 3:e1811. doi: 10.1371/journal.pone.0001811

Mydlarz, L. D., and Jacobs, R. S. (2004). Comparison of an inducible oxidative burst in free-living and symbiotic dinoflagellates reveals properties of the pseudopterosins. *Phytochemistry* 65, 3231–3241. doi: 10.1016/j.phytochem.2004.09.014

Mydlarz, L. D., Jones, L. E., and Harvell, C. D. (2006). Innate immunity, environmental drivers, and disease ecology of marine and freshwater invertebrates. *Annu. Rev. Ecol. Evol. Syst.* 37, 251–288. doi: 10.1146/annurev.ecolsys.37.091305.110103

Nakamura, H., Asari, T., Ohizumi, Y., Kobayashi, J., Yamasu, T., and Murai, A. (1993). Isolation of zooxanthellatoxins, novel vasoconstrictive substances from the zooxanthella *Symbiodinium* sp. *Toxicon* 31, 371–376. doi: 10.1016/0041-0101(93)90172-F

Neely, K. L., and Lewis, C. (2020). Rapid population decline of the pillar coral *Dendrogyra cylindrus* along the Florida Reef Tract. *bioRxiv[Preprint]*. doi: 10.1101/2020.05.09.085886

Neely, K. L., Macaulay, K. A., Hower, E. K., and Dobler, M. A. (2020). Effectiveness of topical antibiotics in treating corals affected by Stony Coral Tissue Loss Disease. *Peer J.* 8:e9289. doi: 10.7717/peerj.9289

Newman, M. C., and Clements, W. H. (2008). *Ecotoxicology: A Comprehensive Treatment*. Boca Raton, FL: CRC Press.

Nürnberger, S., Rentenberger, C., Thiel, K., Schädl, B., Grunwald, I., Ponomarev, I., et al. (2017). Giant crystals inside mitochondria of equine chondrocytes. *Histochem. Cell Biol.* 147, 635–649. doi: 10.1007/s00418-016-1516-6

Owen, R., Knap, A., Ostrander, N., and Carbery, K. (2003). Comparative acute toxicity of herbicides to photosynthesis of coral zooxanthellae. *Bull. Environ. Contam. Toxicol.* 70, 541–548. doi: 10.1007/s00128-003-0020-6

Palmer, C. V., Bythell, J. C., and Willis, B. L. (2011). A comparative study of phenoloxidase activity in diseased and bleached colonies of the coral *Acropora millepora*. *Dev. Comp. Immunol.* 35, 1098–1101. doi: 10.1016/j.dci.2011.04.001

Palmer, C. V., Mydlarz, L. D., and Willis, B. L. (2008). Evidence of an inflammatory-like response in non-normally pigmented tissues of two scleractinian corals. *Proc. R. Soc. Biol. Sci.* 275, 2687–2693. doi: 10.1098/rspb.2008.0335

Palmer, C. V., and Traylor-Knowles, N. G. (2012). Towards an integrated network of coral immune mechanisms. *Proc. R. Soc. B Biol. Sci.* 279, 4106–4114. doi: 10.1098/rspb.2012.1477

Paramasivam, N., Ben-Dov, E., Arotsker, L., Kramarsky-Winter, E., Zvuloni, A., Loya, Y., et al. (2013). Bacterial consortium of *Millepora dichotoma* exhibiting unusual multifocal lesion event in the Gulf of Eilat, Red Sea. *Microb. Ecol.* 65, 50–59. doi: 10.1007/s00248-012-0097-8

Patterson, K. L., Porter, J. W., Ritchie, K. B., Polson, S. W., Mueller, E., Peters, E. C., et al. (2002). The etiology of white pox, a lethal disease of the Caribbean elkhorn coral, *Acropora palmata*. *Proc. Natl. Acad. Sci. U.S.A.* 99, 8725–8730. doi: 10.1073/pnas.092260099

Paxton, C. W., Davy, S. K., and Weis, V. M. (2013). Stress and death of cnidarian host cells play a role in cnidarian bleaching. *J. Exp. Biol.* 216, 2813–2820. doi: 10.1242/jeb.087858

Peters, E. C. (2015). "Diseases of coral reef organisms," in *Coral Reefs in the Anthropocene*, ed. C. Birkeland (Dordrecht: Springer Netherlands), 147–178. doi: 10.1007/978-94-017-7249-5_8

Peters, E. C. (2016). "Anatomy," in *Diseases of Coral*, eds C. M. Woodley, C. A. Downs, A. W. Bruckner, J. W. Porter, and S. B. Galloway (Hoboken, NJ: John Wiley & Sons Inc), 85–107.

Porter, J. W., Dustan, P., Jaap, W. C., Patterson, K. L., Kosmynin, V., Meier, O. W., et al. (2001). Patterns of spread of coral disease in the Florida Keys. *Hydrobiology* 460, 1–24. doi: 10.1007/978-94-017-3284-0_1

Precht, W. F., Gintert, B. E., Robbart, M. L., Fura, R., and van Woesik, R. (2016). Unprecedented disease-related coral mortality in southeastern Florida. *Sci. Rep.* 6:31374. doi: 10.1038/srep31374

Price, K. L., and Peters, E. C. (2018). *Histological Techniques for Corals*. Available online at: https://www.amazon.com/Histological-Techniques-Corals-Kathy-Price-ebook/dp/B07L1DSCYZ

Quintero-Hunter, I., Grier, H., and Muscato, M. (1991). Enhancement of histological detail using metanil yellow as a counter-stain in periodic acid Schiff's hematoxylin staining of glycol methacrylate tissue sections. *Biotech. Histochem.* 66, 169–172. doi: 10.3109/10520299109109964

Ramos-Silva, P., Kaandorp, J., Huisman, L., Marie, B., Zanella-Cleon, I., Guichard, N., et al. (2013). The skeletal proteome of the coral *Acropora millepora*: the evolution of calcification by co-option and domain shuffling. *Mol. Biol. Evol.* 30, 2099–2112. doi: 10.1093/molbev/mst109

Raz-Bahat, M., Douek, J., Moiseeva, E., Peters, E. C., and Rinkevich, B. (2017). The digestive system of the stony coral *Stylophora pistillata*. *Cell Tissue Res.* 368, 311–323. doi: 10.1007/s00441-016-2555-y

Reichelt-Brushett, A. J., and McOrist, G. (2003). Trace metals in the living and nonliving components of scleractinian corals. *Mar. Pollut. Bull.* 46, 1573–1582. doi: 10.1016/S0025-326X(03)00323-0

Reynolds, E. S. (1963). The use of lead citrate at high pH as an electron-opaque stain in electron microscopy. *J. Cell Biol.* 17, 208–212. doi: 10.1083/jcb.17.1.208

Richardson, L. L. (1998). Coral diseases: what is really known? *Trends Ecol. Evol.* 13, 438–443. doi: 10.1016/S0169-5347(98)01460-8

Richardson, L. L., Goldberg, W. M., Carlton, R. G., and Halas, J. C. (1998a). Coral disease outbreak in the Florida Keys: plague type II. *Rev. Biol. Trop.* 46(Suppl. 5), 187–198.

Richardson, L. L., Goldberg, W. M., Kuta, K. G., Aronson, R. B., Smith, G. W., Ritchie, K. B., et al. (1998b). Florida's mystery coral-killer identified. *Nature* 392, 557–558. doi: 10.1038/33302

Rippe, J. P., Kriefall, N. G., Davies, S. W., and Castillo, K. D. (2019). Differential disease incidence and mortality of inner and outer reef corals of the upper Florida Keys in association with a white syndrome outbreak. *Bull. Mar. Sci.* 95, 305–316. doi: 10.5343/bms.2018.0034

Ritchie, K. (2011). "Bacterial symbionts of corals and *Symbiodinium*," in *Beneficial Microorganisms in Multicellular Life Forms*, eds E. Rosenberg and U. Gophna (Berlin: Springer-Verlag), 139–150. doi: 10.1007/978-3-642-21680-0

Rodríguez-Villalobos, J. C., Work, T. M., Calderon-Aguilera, L. E., Reyes-Bonilla, H., and Hernández, L. (2015). Explained and unexplained tissue loss in corals from the tropical eastern Pacific. *Dis. Aquat. Org.* 116, 121–131. doi: 10.3354/dao02914

Rogers, C. S. (1990). Responses of coral reefs and reef organisms to sedimentation. *Mar. Ecol. Prog. Ser.* 62, 185–202. doi: 10.3354/meps062185

Rosales, S. M., Clark, A. S., Huebner, L. K., Ruzicka, R. R., and Muller, E. M. (2020). Rhodobacterales and Rhizobiales are associated with stony coral tissue loss disease and its suspected sources of transmission. *Front. Microbiol.* 11:681. doi: 10.3389/fmicb.2020.00681

Rosenberg, E. (2004). "The bacterial disease hypothesis of coral bleaching," in *Coral Health and Disease*, eds E. Rosenberg and Y. Loya (Berlin: Springer), 445–461. doi: 10.1007/978-3-662-06414-6_25

Russell, G., Stewart, J., and Haig, D. (2008). Malignant catarrhal fever: a review. *Vet. J.* 179, 324–335. doi: 10.1016/j.tvjl.2007.11.007

Santavy, D. L., Mueller, E., Peters, E. C., MacLaughlin, L., Porter, J. W., Patterson, K. L., et al. (2001). Quantitative assessment of coral diseases in the Florida keys: strategy and methodology. *Hydrobiol.* 460, 39–52. doi: 10.1007/978-94-017-3284-0_3

Sassi, R., Sassi, C. F. C., Gorlach-Lira, K., and Fitt, W. K. (2015). Pigmentation changes in *Siderastrea* spp. *during bleaching events in the coastal reefs of northeastern Brazil*. *Latin Amer. J. Aquat. Res.* 43, 176–185. doi: 10.3856/vol43-issue1-fulltext-15

Soffer, N., Brandt, M. E., Correa, A. M. S., Smith, T. B., and Thurber, R. V. (2014). Potential role of viruses in white plague coral disease. *ISME J.* 8, 271–283. doi: 10.1038/ismej.2013.137

Sunagawa, S., DeSantis, T. Z., Piceno, Y. M., Brodie, E. L., DeSalvo, M. K., Voolstra, C. R., et al. (2009a). Bacterial diversity and white plague disease-associated community changes in the Caribbean coral *Montastraea faveolata*. *ISME J.* 3, 512–521. doi: 10.1038/ismej.2008.131

Sunagawa, S., Wilson, E. C., Thaler, M., Smith, M. L., Caruso, C., Pringle, J. R., et al. (2009b). Generation and analysis of transcriptomic resources for a model system on the rise: the sea anemone *Aiptasia pallida* and its dinoflagellate endosymbiont. *BMC Genomics* 10:258. doi: 10.1186/1471-2164-10-258

Sutherland, K. P., Berry, B., Park, A., Kemp, D. W., Kemp, K. M., Lipp, E. K., et al. (2016). Shifting white pox aetiologies affecting *Acropora palmata* in the Florida Keys, 1994–2014. *Phil. Trans. R. Soc. B* 371:20150205. doi: 10.1098/rstb.2015.0205

Thrusfield, M. (2016). "Etiology," in *Diseases of Coral*, eds C. M. Woodley, C. A. Downs, A. W. Bruckner, J. W. Porter, and S. B. Galloway (Hoboken, NJ: John Wiley & Sons Inc), 16–27.

Upton, S. J., and Peters, E. C. (1986). A new and unusual species of coccidium (Apicomplexa: Agamococcidiorida) from Caribbean scleractinian corals. *J. Invertebr. Pathol.* 47, 184–193. doi: 10.1016/0022-2011(86)90045-5

Verde, A., Bastidas, C., and Croquer, A. (2016). Tissue mortality by Caribbean ciliate infection and white band disease in three reef-building coral species. *PeerJ* 4:e2196. doi: 10.7717/peerj.2196

Wagner, D. E., Kramer, P., and Van Woesik, R. (2010). Species composition, habitat, and water quality influence coral bleaching in southern Florida. *Mar. Ecol. Prog. Ser.* 408, 65–78. doi: 10.3354/meps08584

Walton, C. J., Hayes, N. K., and Gilliam, D. S. (2018). Impacts of a regional, multi-year, multi-species coral disease outbreak in southeast Florida. *Front. Mar. Sci.* 5:323. doi: 10.3389/fmars.2018.00323

Weil, E. (2004). "Coral reef diseases in the wider Caribbean," in *Coral Health and Disease*, eds E. Rosenberg and Y. Loya (Berlin: Springer), 35–68. doi: 10.1007/978-3-662-06414-6_2

Weil, E., Hernández-Delgado, E. A., Gonzalez, M., Williams, S., Suleimán-Ramos, S., Figuerola, M., et al. (2019). Spread of the new coral disease "SCTLD" into the Caribbean: implications for Puerto Rico. *Reef Encounter* 34, 38–43.

Weis, V. M. (2008). Cellular mechanisms of cnidarian bleaching: stress causes the collapse of symbiosis. *J. Exp. Biol.* 211, 3059–3066. doi: 10.1242/jeb.009597

Weis, V. M., Davy, S. K., Hoegh-Guldberg, O., Rodriguez-Lanetty, M., and Pringle, J. R. (2008). Cell biology in model systems as the key to understanding corals. *Trends Ecol. Evol.* 23, 369–376. doi: 10.1016/j.tree.2008.03.004

Wietheger, A., Starzak, D. E., Gould, K. S., and Davy, S. K. (2018). Differential ROS generation in response to stress in *Symbiodinium* spp. *Biol. Bull.* 234, 11–21. doi: 10.1086/696977

Williams, D. E., and Miller, M. W. (2012). Attributing mortality among drivers of population decline in *Acropora palmata* in the Florida Keys (USA). *Coral Reefs* 31, 369–382. doi: 10.1007/s00338-011-0847-y

Williams, G. J., Work, T. M., Aeby, G. S., Knapp, I. S., and Davy, S. K. (2011). Gross and microscopic morphology of lesions in Cnidaria from Palmyra Atoll. *Central Pacific. J. Invertebr. Pathol.* 106, 165–173. doi: 10.1016/j.jip.2010.08.002

Wilson, W. H., Dale, A. L., Davy, J. E., and Davy, S. K. (2005). An enemy within? Observations of virus-like particles in reef corals. *Coral Reefs* 24, 145–148. doi: 10.1007/s00338-004-0448-0

Woodley, C. M., Bruckner, A. W., McLenon, A. L., Higgins, J. L., Galloway, S. B., and Nicholson, J. H. (2008). *Field Manual for Investigating Coral Disease Outbreaks. NOAA Technical memorandum NOS NCCOS* 80 and CRCP 6. Silver Spring, MD: National Oceanic and Atmospheric Administration.

Work, T., and Meteyer, C. (2014). To understand coral disease, look at coral cells. *Ecohealth* 11, 610–618. doi: 10.1007/s10393-014-0931-1

Work, T. M., and Aeby, G. S. (2006). Systematically describing gross lesions in corals. *Dis. Aquat. Org.* 70, 155–160. doi: 10.3354/dao070155

Work, T. M., and Aeby, G. S. (2011). Pathology of tissue loss (white syndrome) in *Acropora* sp. corals from the Central Pacific. *J. Invertebr. Pathol.* 107, 127–131. doi: 10.1016/j.jip.2011.03.009

Work, T. M., Russell, R., and Aeby, G. S. (2012). Tissue loss (white syndrome) in the coral *Montipora capitata* is a dynamic disease with multiple host responses

and potential causes. *Proc. R. Soc. B Biol. Sci.* 279, 4334–4341. doi: 10.1098/rspb.2012.1827

Wright, R. M., Kenkel, C. D., Dunn, C. E., Shilling, E. N., Bay, L. K., and Matz, M. V. (2017). Intraspecific differences in molecular stress responses and coral pathobiome contribute to mortality under bacterial challenge in *Acropora millepora*. *Sci. Rep.* 7:2609. doi: 10.1038/s41598-017-02685-1

Zhou, Z., Zhao, S., Tang, J., Liu, Z., Wu, Y., Wang, Y., et al. (2019). Altered immune landscape and disrupted coral–*Symbiodinium* symbiosis in the scleractinian coral *Pocillopora damicornis* by *Vibrio coralliilyticus* challenge. *Front. Physiol.* 10:366. doi: 10.3389/fphys.2019.00366

Conflict of Interest: The authors declare that the research was conducted in the absence of any commercial or financial relationships that could be construed as a potential conflict of interest.